AD/A-000 952

PHASED-ARRAY ANTENNA ANALYSIS FOR PACIFIC MISSILE RANGE INSTRUMENTATION AIRCRAFT

J. B. L. Rao, et al

Naval Research Laboratory
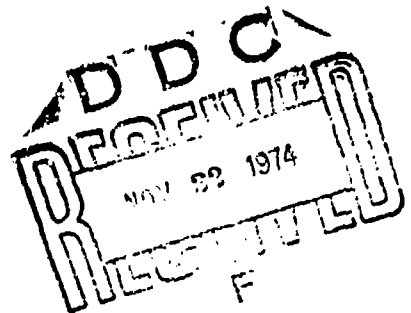Washington, D. C.

15 October 1974

AD A000952

Phased-Array Antenna Analysis for PMR Instrumentation Aircraft

J. B. L. RAO AND J. K. HSIAO

Search Radar Branch
Radar Division

October 15, 1974

NOV 22 1974

NAVAL RESEARCH LABORATORY
Washington, D.C.

60

REPORT DOCUMENTATION PAGE		READ INSTRUCTIONS BEFORE COMPLETING FORM
1. REPORT NUMBER NRL Report 7806	2. GOVT ACCESSION NO.	3. RECIPIENT'S CATALOG NUMBER AD/A-000 951
4. TITLE (and Subtitle) PHASED-ARRAY ANTENNA ANALYSIS FOR PACIFIC MISSILE RANGE INSTRUMENTATION AIRCRAFT		5. TYPE OF REPORT & PERIOD COVERED An interim report on a continuing NRL problem.
		6. PERFORMING ORG. REPORT NUMBER
7. AUTHOR(s) J.B.L. Rao and J.K. Hsiao		8. CONTRACT OR GRANT NUMBER(s)
9. PERFORMING ORGANIZATION NAME AND ADDRESS Naval Research Laboratory Washington, D.C. 20375		10. PROGRAM ELEMENT, PROJECT, TASK AREA & WORK UNIT NUMBERS NRL Problem R02-24 A-5355352-652E-4F0990500C
11. CONTROLLING OFFICE NAME AND ADDRESS Department of the Navy Naval Air Systems Command Washington, D.C. 20361		12. REPORT DATE October 15, 1974
		13. NUMBER OF PAGES 59
14. MONITORING AGENCY NAME & ADDRESS(if different from Controlling Office)		15. SECURITY CLASS. (of this report)
		15a. DECLASSIFICATION/DOWNGRADING SCHEDULE

16. DISTRIBUTION STATEMENT (of this Report)

Approved for public release; distribution unlimited.

17. DISTRIBUTION STATEMENT (of the abstract entered in Block 20, if different from Report)

19. KEY WORDS (Continue on reverse side if necessary and identify by block number)

Conformal arrays
Phased arrays
Steering methods
Radiation patterns

20. ABSTRACT (Continue on reverse side if necessary and identify by block number)

Conformal phased arrays for Extended Area Tracking System (EATS), Target Control System (TCS), and Telemetry System (TMS) are analyzed using computer simulation when they are located on a P-3 aircraft. First, the radiation patterns are obtained by assuming that the array elements are uniformly spaced around the curved surface, and the exact phase is used to scan the beams. To simplify the phase control, a method is discussed by which the phase control is approximated by a planar array, row-column steering. The radiation patterns are obtained using the approximate technique and compared with those obtained by using correct phase control. The results indicate

DD FORM 1473 1 JAN 73 EDITION OF 1 NOV 65 IS OBSOLETE
S/N 0102-014-6601

i

20.

that the approximate phasing can be used with EATS and TCS arrays with negligible degradation in array performance. For TMS arrays, the simple row-column steering introduces unacceptable phase errors. For such arrays, a modified approximate phasing is recommended.

CONTENTS

PHASED ARRAY ANTENNA ANALYSIS FOR
PACIFIC MISSILE RANGE INSTRUMENTATION AIRCRAFT

INTRODUCTION

Advanced Surface Missile Defense (ASMD) and other program requirements necessitate implementation of an extended-area instrumentation system at the Pacific Missile Range (PMR) that will employ relay aircraft for tracking, telemetry, and target control relay functions for multiple-object operations in areas not covered by existing land instrumentation. Phased-array receiving antennas are being considered for the range instrumentation aircraft for reception of relatively low-power signals. The arrays have been assumed to be conformal with the existing P-3 aircraft surfaces. The purpose of this report is to provide information on realizable performance and potential problems associated with such conformal arrays.

To analyze the conformal arrays, a general computer program was developed that computes the array pattern, gain and polarization of the radiating fields at all scan angles as required by the PMR system. The program is formulated in such a general way that the array size, location, element spacing, and the curvature of the conformal surface can be varied with minimum changes in the program. Using this computer program, we obtained the radiation patterns for the Extended Area Tracking System (EATS), Target Control System (TCS), and Telemetry System (TMS) receiving arrays as located on P-3 aircraft. The required coverage is assumed to be $\pm 60°$ in azimuth and $\pm 15°$ in elevation. First, the radiation patterns are obtained by assuming that the array elements are uniformly spaced around the curved surface, and that exact phasing is used to scan the beams. However, the required hardware and software are very costly for obtaining exact phases for each element and for every scan angle. Therefore, a study was made to investigate possible methods of phasing that will simplify the required hardware. A method is discussed by which the phase control is approximated by a planar array, row-column steering. The radiation patterns are obtained with this approximate technique and compared with those obtained by using correct steering phases. The results are presented for EATS, TCS, and TMS arrays when they are located on the fuselage, and for EATS and TCS when they are located on the vertical stabilizer. The results presented in this report indicate that the planar array, row-column steering technique can be used with EATS and TCS arrays with no noticeable degradation in their performance. The same technique can be used for TMS arrays of 32 X 1 elements with negligible degradation when scanned to $15°$ in elevation. However, the simple planar phasing technique may introduce unacceptable phase errors for larger TMS arrays or when scanned to $60°$ in azimuth. For such arrays, an extension of the simple phasing technique is suggested.

Note: Manuscript was submitted July 30, 1974.

1

SIMPLIFIED TECHNIQUE FOR SCANNING OF CONFORMAL ARRAYS

To steer the beam of a conformal array on a general surface, it is first necessary to calculate the required phase for each element and each scan angle. Once calculated, it has to be practically implemented. The complexity of the hardware needed to scan the beams of conformal phased arrays increases greatly as the surface geometry becomes more complex. This control of element phases is one of the most important problems to be overcome in implementing conformal arrays. Here, an approximate technique for controlling the phase of a conformal array on a general surface will be discussed first. An equation is obtained for the phase errors introduced by the approximate technique, as a function of array parameters and the required scan angles. This equation will be used later in the report to estimate the phase errors introduced by using the approximate technique for the specific arrays under consideration.

Consider elements of a general conformal array phased in such a way that the wave emanating from the array is a plane wave traveling in a given direction. This can be thought of as a projection of the elements on some plane surface as shown in Fig. 1.
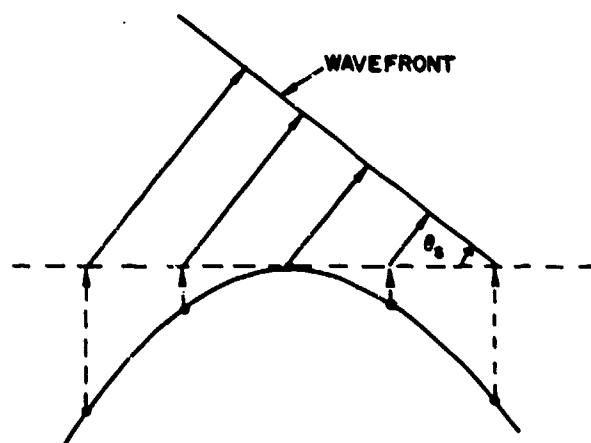

Fig. 1 — Geometry of conformal array whose elements
are projected onto a plane surface

By judiciously placing the elements on the curved surface, the projected element positions will have uniform distribution. In the two-dimensional case shown in Fig. 1, we now have the equivalent of a linear array in the projected plane. Now the beam may be scanned by using the simpler, well-known technique of the equally spaced linear array. The Simplicity of scanning an equally spaced linear array lies in the fact that the phase difference needed between any two adjacent elements is the same for any given scan angle. Therefore, only one value is needed to find the excitation phase of all elements in the linear array. This can be implemented by a simple adder. For a conformal array, no such simple relation exists between the element excitations. It is necessary to compute the excitation phase for each element and for every scan angle. Implementing this computation requires complex hardware and software. Thus, by using the approximate technique, a reduction in the hardware and software can be achieved. However, there will be some phase errors introduced by the approximate technique. Equations for these phase errors will

2

be obtained next for the arrays on known conformal geometries such as the circular arc and the circular cylinder.

Consider a circular arc array as shown in Fig. 2. Let the elements be distributed along the circular arc in such a manner that the projected element positions will have uniform interelement spacing of d. Let R be the radius of curvature of the circular arc.
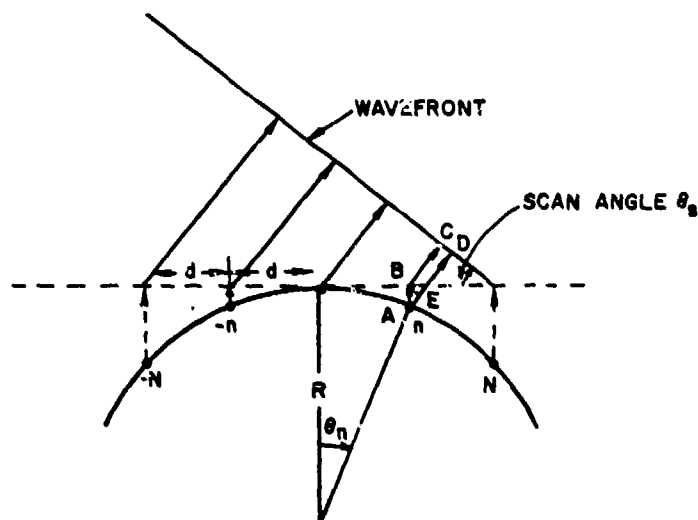

Fig. 2 — Geometry of a circular arc array whose elements are projected onto a plane surface

The nth element position on the arc is specified by the angle θ_n, and it is assumed that there are $2N + 1$ elements in the array. To steer the beam of this circular arc array to an angle θ_s, the correct phase required at each element should correspond to the path length between each element and the wavefront. For the nth element this corresponds to the path length AD. In the approximate technique, this is approximated by a path length $AB + BC$. The path length AB is a constant (independent of scan angle) for a given element, and the path length BC corresponds to the linear array phase needed to scan the beam to an angle θ_s. Therefore, the path-length errors introduced by the approximate technique are the difference between path lengths $(AB + BC)$ and AD, which is the same as $AB - AE$. Therefore, the phase error in the nth element is given by (see Fig. 2).

$$\epsilon_n = \frac{2\pi}{\lambda}(AB-AE) = \frac{2\pi}{\lambda} AB(1-\cos\theta_s)$$

$$= \frac{2\pi}{\lambda} R(1-\cos\theta_n)(1-\cos\theta_s).$$

(1)

The phase error given by Eq. (1) is present for the element whose position is specified by $-\theta_n$. Hence, the phase errors are symmetric and will not effect the main-beam pointing direction.

3

The procedure used in obtaining Eq. (1) can be extended to an array on a circular cylinder, as shown in Fig. 3. Here, each column corresponds to an arc array, and each row is an equally spaced linear array. Similar to the circular arc array, the elements in each column are judiciously placed so that when projected onto the xy-plane they have uniform distribution. We now have the equivalent of a planar array in the projected plane (xy-plane). Now, the beam may be scanned by using the simpler, well known row-column steering of the uniformly spaced planar array. Thus, by using the approximate technique, a reduction in hardware and software can be achieved. Following the procedure used for circular arc arrays, it can be shown that the phase errors in each column (circular arc) of the array on circular cylinder is given by

$$\epsilon_n = \frac{2\pi R}{\lambda} (1-\cos\theta_s\cos\varphi_s)(1-\cos\theta_n)$$ (2)

where θ_s and φ_s are the elevation and azimuth scan angles, R is the radium of curvature, and θ_n is the element angular position from the yz-plane. Eq. (2) is similar to Eq. (1) except for the additional factor of $\cos\varphi_s$, which accounts for the effect of scanning in the φ plane. Since Eq. (1) is a special case of Eq. (2) when $\varphi_s = 0$, the remaining discussion is addressed to Eq. (2).
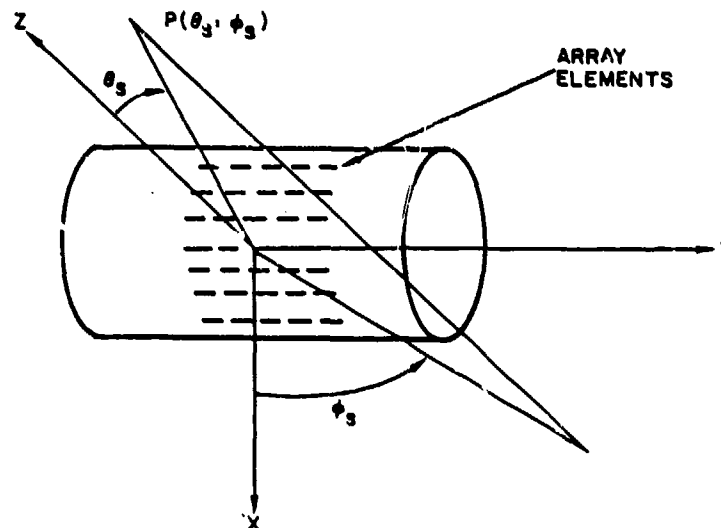
Fig. 3 — Geometry of a conformal array on a
circular cylinder

From Eq. (2) it is clear that for a given set of array parameters (R and θ_n), the phase errors will increase with the increase in scan angles θ_s and φ_s. Also, the element phase error depends on where the element is located (θ_n) in the array. It is clear from Eq. (2) that the phase error in the central element ($\theta_n = \theta_o = 0$) is zero and the error increases as the element angular separation θ_n from the broad side increases. Therefore, the maximum phase errors occur in the end elements. Since the phase errors are not the same in each element, the rms phase error will give more insight into the effect of phase

4

errors than the absolute phase error in each element. The phase error for a discrete array can be represented by

$$\epsilon_{rms} = \frac{1}{N}\sqrt{\sum_{1}^{N}\epsilon_n^2} \tag{3}$$

where ϵ_n is given by Eq. (2) and N is half the number of elements in the array (except the center element).

If the elements are not too widely spaced, the summation in Eq. (3) can be accurately represented by an integration as

$$\epsilon_{rms} = \sqrt{\frac{1}{\theta_N}\int_0^{\theta_N}\epsilon_n^2 d\theta_n}. \tag{4}$$

Substituting for ϵ_n from Eq. (2) into Eq. (4) shows that

$$\epsilon_{rms} = \frac{2\pi R}{\lambda}(1-\cos\theta_s\cos\varphi_s)\sqrt{1.5-\frac{2\sin\theta_N}{\theta_N}+\frac{\sin 2\theta_N}{4\theta_N}}. \tag{5}$$

Equations (2) and (5) are used to find the phase errors introduced by row-column steering for EATS and TCS arrays and for the specified scan angles. The results are given later in the appropriate sections. For larger arrays and wider scan angles, the phase errors introduced by simple row-column steering may be unacceptable. For such arrays, a modified method is suggested. In the modified method, the conformal array is divided into several subarrays or arcs, as shown in Fig. 4, and each subarray is treated as a separate array in applying the row-column steering discussed earlier. This modified method is still under investigation, and the results will be published in a separate report.

ARRAYS LOCATED ON FUSELAGE

In this report the primary attention is given to the arrays located on P-3 aircraft fuselage. For the P-3 aircraft, the shape of the fuselage is mainly a circular cylinder [1] with a radius of curvature of 60 in.; the cylindrical surface extends from fuselage station 306 to 901 (fuselage station numbers are given in inches). The position of the wings on the fuselage occupy the stations from 570 to 695. Therefore, the position on the fuselage where the arrays could be located is a circular cylinder. Hence, the following discussion is primarily concerned with the performance of the arrays on a circular cylinder.

5
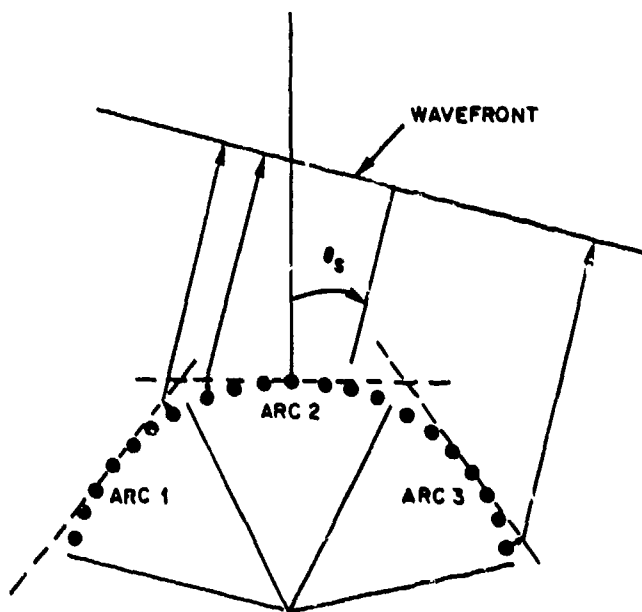
Fig. 4 — Extension of planar array phasing for larger conformal arrays

On such structures, the array elements are usually distributed uniformly. To scan such arrays it is necessary to calculate the phase angle for each element and each scan angle. Implementing this requires complex and costly hardware. To simplify the hardware requirement, a study is made to determine the possibility of using familiar planar array, row-column steering for the arrays on the circular cylinder. The results presented in the previous section show that the row-column steering could be used if the scanning requirements and array size are such that the phase errors introduced are negligible and the elements are judiciously located on the curved surface (in such a manner that, when projected onto a plane, they will have uniform spacing). The results obtained by this row-column steering (sometimes called approximate phasing) are compared with the results obtained by exact phasing. In what follows, the results are discussed for each array. For all the arrays on the fuselage it is assumed that the individual elements have the pattern of a horizontal dipole. This will have the effect of reducing the side-lobe levels in the azimuth plane and thereby reducing the effect of scattering by wings, engines, and other obstacles.

EATS Array

The size of the EATS array is assumed to be 1m X 2m (as recommended in Ref. [2], which translates to a 3λ X 6λ array at 900 MHz. The smaller dimension is assumed to be along the curved surface.

5 X 10 Element Array — In Ref. [2] it is proposed that a 5 X 10 element array be used for EATS. Therefore, it is analyzed first. The radiation patterns are obtained first by assuming that the array elements are distributed uniformly in a rectangular grid on P-3 aircraft fuselage, and the exact phasing is used in scanning. The results are shown in Figs. 5a through 5e. Figures 5a and 5b show the elevation patterns when scanned to 0° and 15°, respectively, in the elevation plane. Figures 5c through 5e show the azimuth patterns scanned to 0°, 30°, and 60° in the azimuth plane. The step changes in the elevation patterns in Figs. 5a and 5b and other elevation patterns presented later in this report are caused by a provision in the computer program. This provision makes it possible to drop the element contribution whenever the element becomes invisible (because of the curved surface) from the point at which the radiation field is being computed. Figures 5a through 5e show that the side-lobe levels are high in the elevation patterns and that grating lobes appeared in the azimuth patterns when scanned to 60°. These undesirable characteristics are caused by the larger interelement spacing (spacing in elevation plane is ≈0.75λ and in the azimuth plane it is 0.667λ). For the scanning range of interest, it is possible to use these larger interelement spacings and still avoid grating lobes or high side lobes if a planar array arranged in a triangular grid is used [3]. We therefore presume that in Ref. [2] the authors assumed a planar array with triangular grid in recommending wider interelement spacings. However, it will be shown that the triangular grid on a circular cylinder may not be as effective.
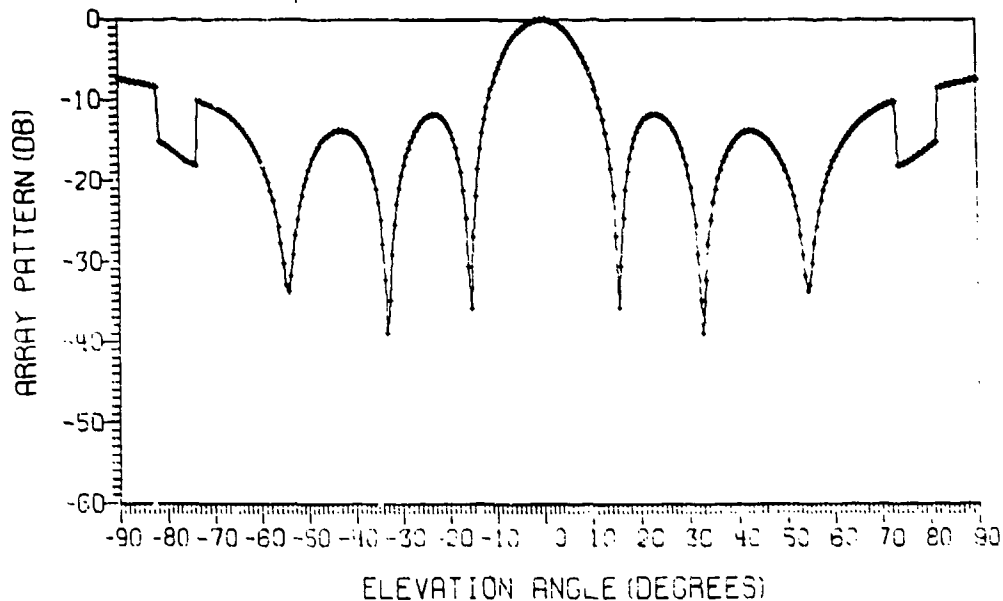
Fig. 5a — Elevation pattern of 5 X 10 rectangular grid EATS array located on fuselage

Fig. 5b — Elevation pattern of 5 × 10 rectangular grid EATS array located on fuselage and scanned to 15° in elevation

Fig. 5c — Azim. th pattern of 5 × 10 rectangular grid EATS array located on fuselage

8

Fig. 5d — Azimuth pattern of 5 × 10 rectangular grid EATS array located on fuselage
and scanned to 30° in azimuth

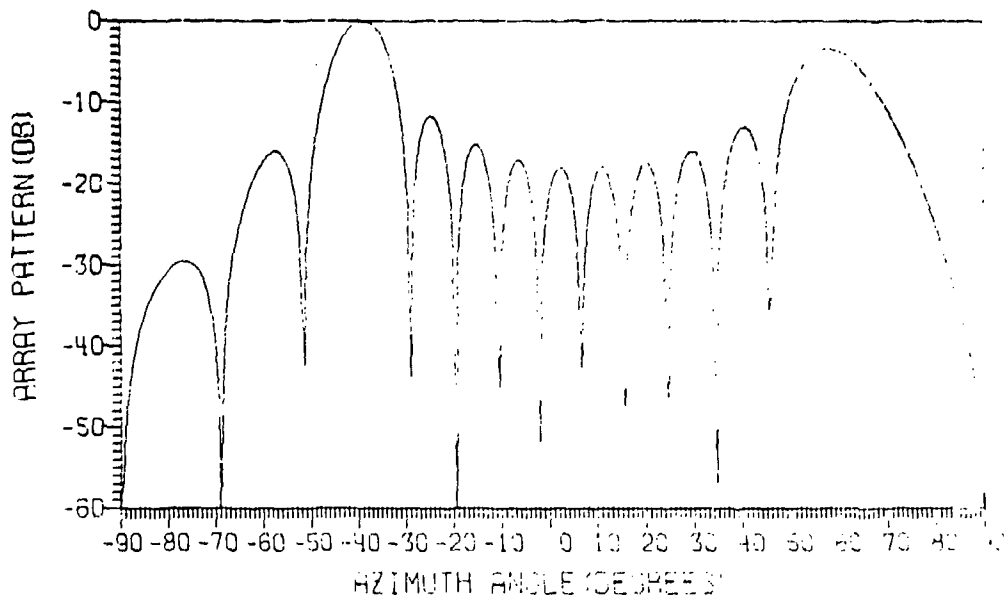Fig. 5e — Azimuth of 5 × 10 rectangular grid EATS array located on fuselage
and scanned to 60° in azimuth

9

The arrangement of the triangular grids considered is shown in Figs. 6 and 7. In Fig. 6 the interelement spacing in each column is assumed to be 0.75λ and the row spacing is assumed to be 0.667λ. There are 10 columns in the array, and each column contains either 5 or 4 elements, as shown in Fig. 6. The computed radiation patterns are shown in Figs. 8a through 8e. From these patterns we note that using the triangular grid of Fig. 6 has the effect of reducing the side lobes in the elevation plane to reasonable levels compared to Figs. 5a through 5e. However, the grating lobes still appear in the azimuth plane when the beam is scanned to 60° in azimuth. It is possible to eliminate the grating lobes in the azimuth plane by using a triangular grid array, as shown in Fig. 7, with 50 elements. The difference between the triangular grid arrays of Figs. 6 and 7 is that the effective interelement spacing is smaller than λ/2 in the elevation plane for Fig. 6 and in the azimuth plane for Fig. 7. The patterns for the triangular grid array of Fig. 7 are shown in Figs. 9a through 9e. Note from these figures that the grating lobes in the azimuth plane are eliminated. However, the side lobes in the elevation plane are considerably high when scanned to 15° in elevation. Therefore, it is clear that the interelement spacings recommended in Ref. [2] cannot be used for the arrays on the circular cylinder if the requirements include no grating lobes and reasonable side-lobe levels.
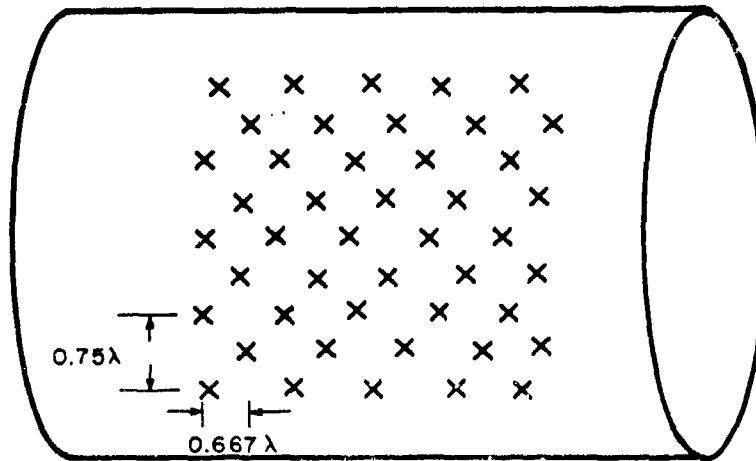
Fig. 6 — Triangular grid arrangement 1 of EATS array
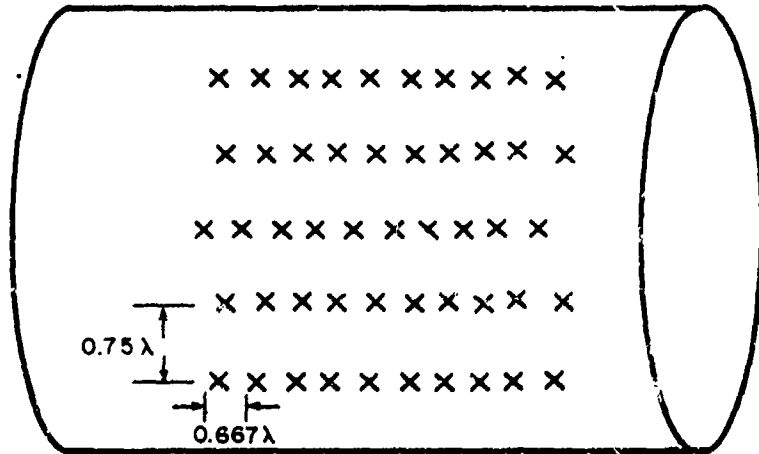
Fig. 7 — Triangular grid arrangement 2 of EATS array
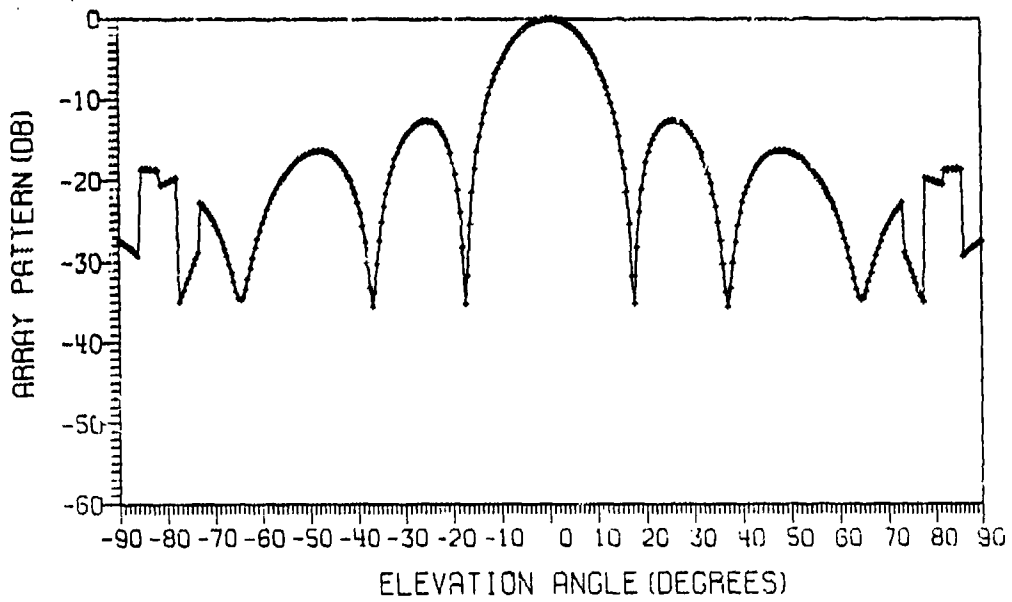
Fig. 8a — Elevation pattern of triangular grid (Fig. 6) EATS array located on fuselage
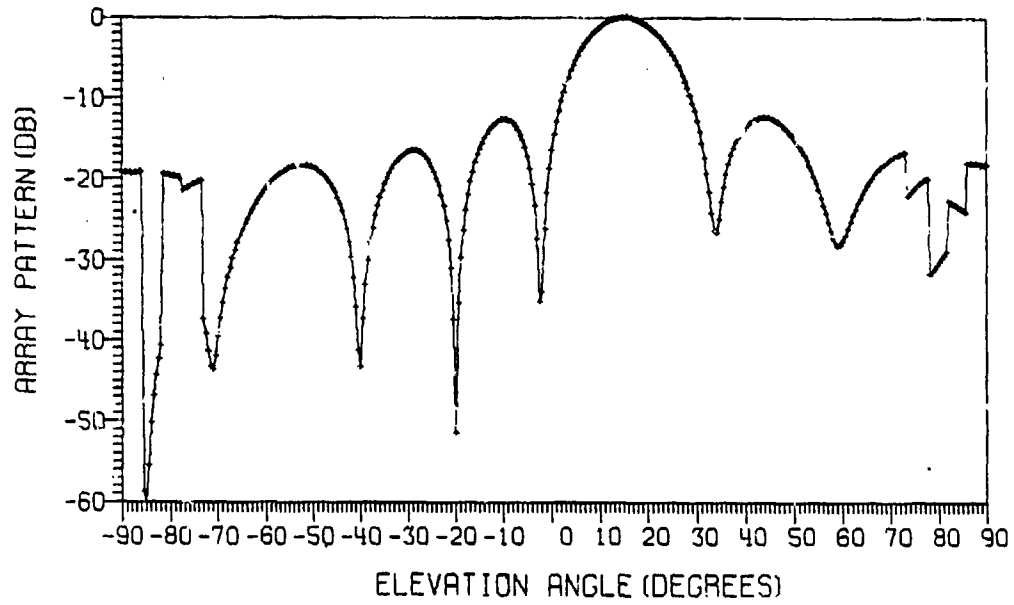
Fig. 8b — Elevation pattern of triangular grid (Fig. 6) EATS array located on fuselage
and scanned to 15° in elevation
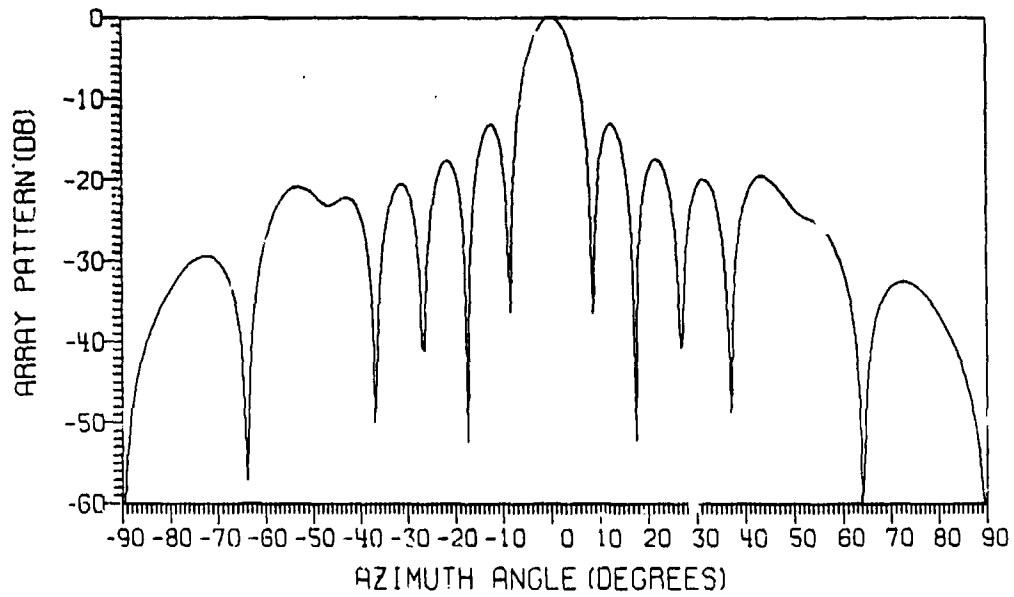
Fig. 8c — Azimuth pattern of triangular grid (Fig. 6) EATS array located on fuselage
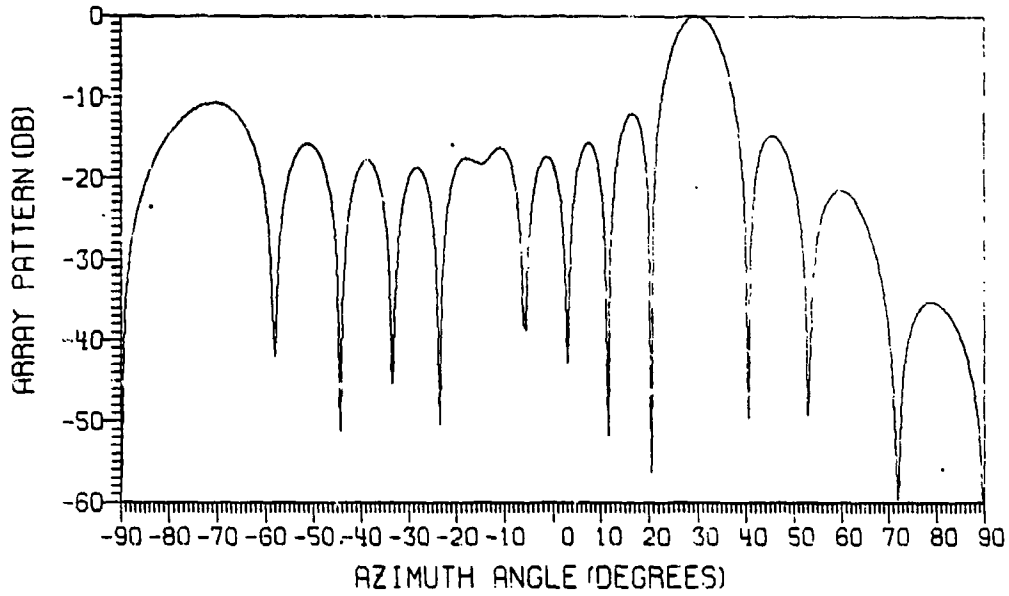
Fig. 8d — Azimuth pattern of triangular grid (Fig. 6) EATS array located on fuselage
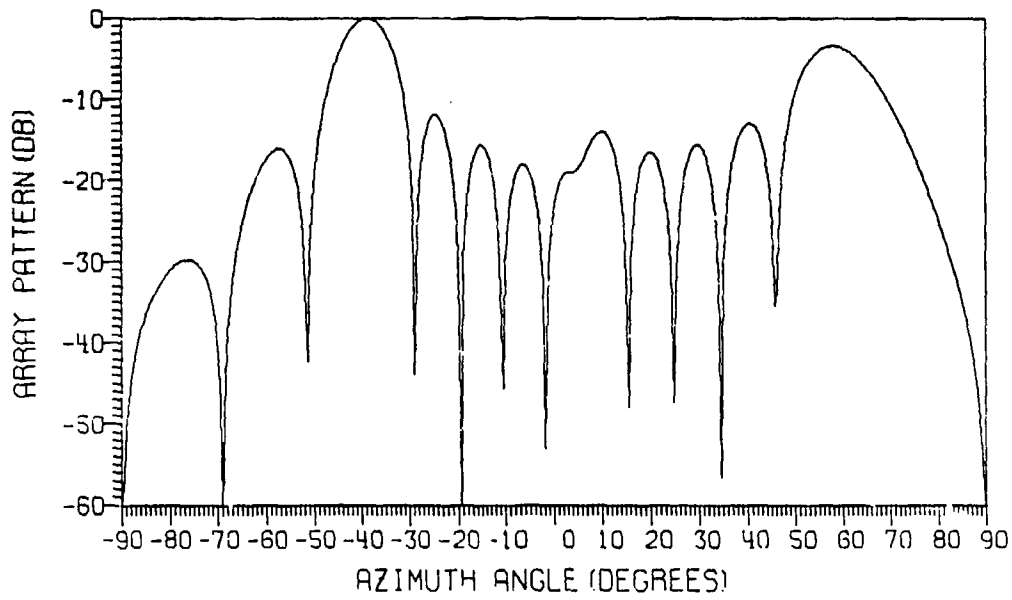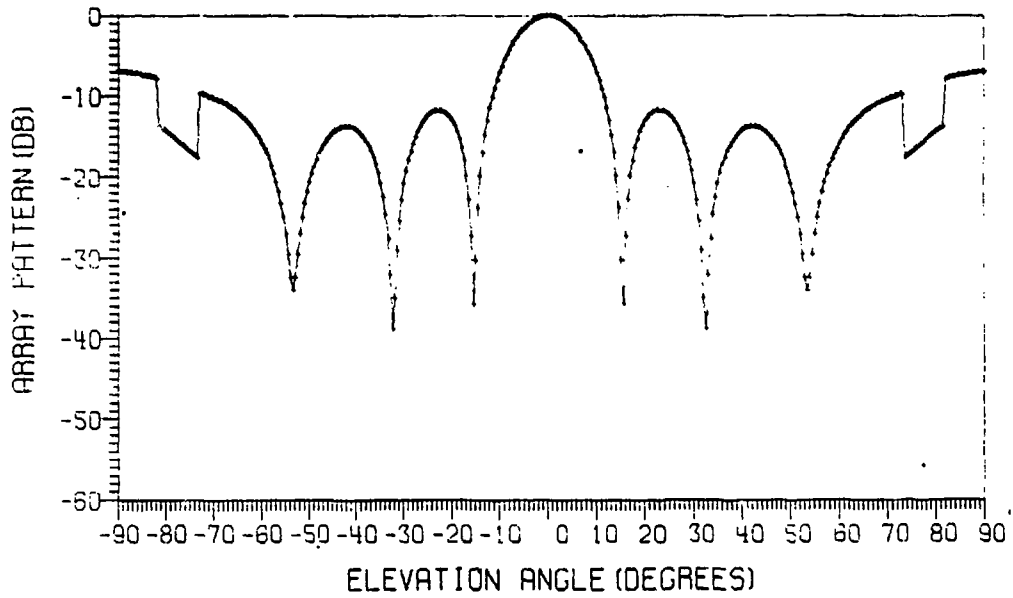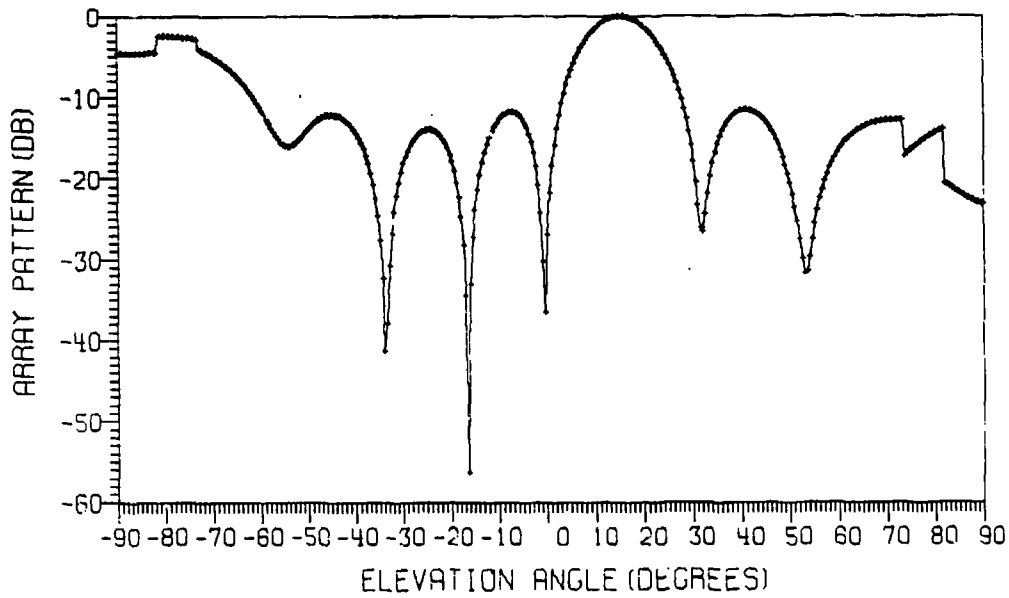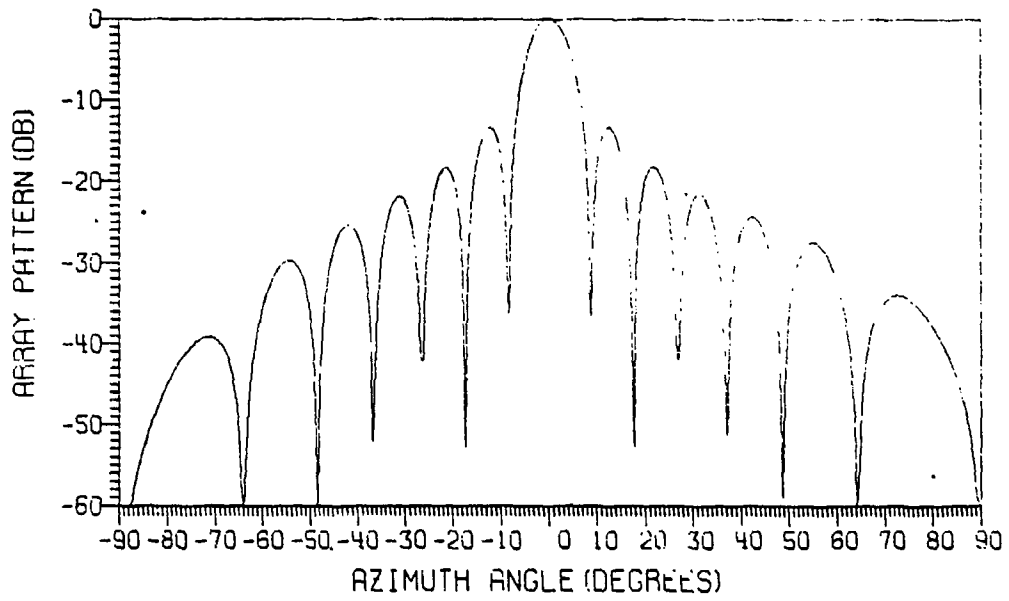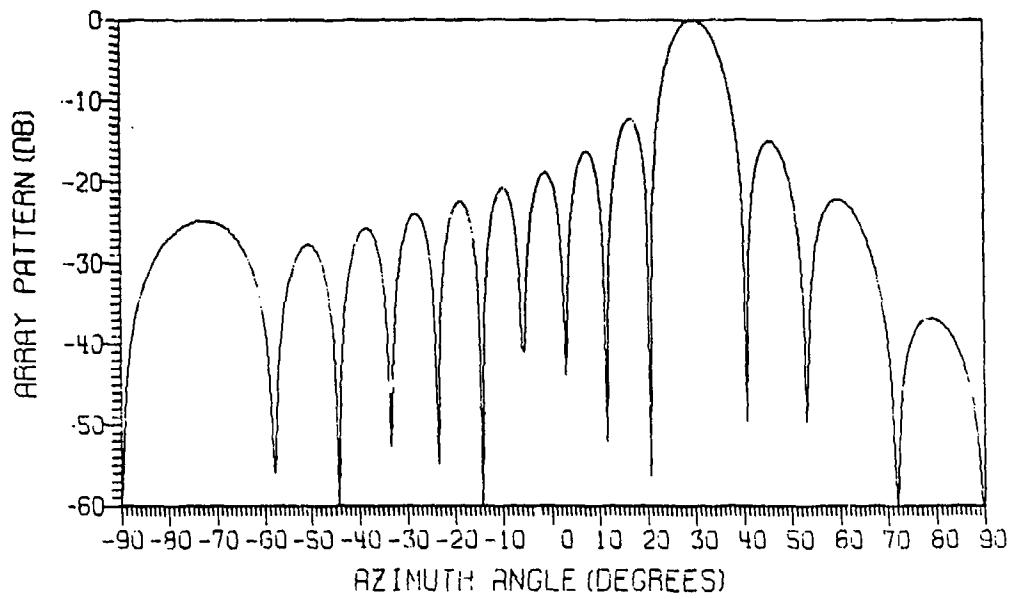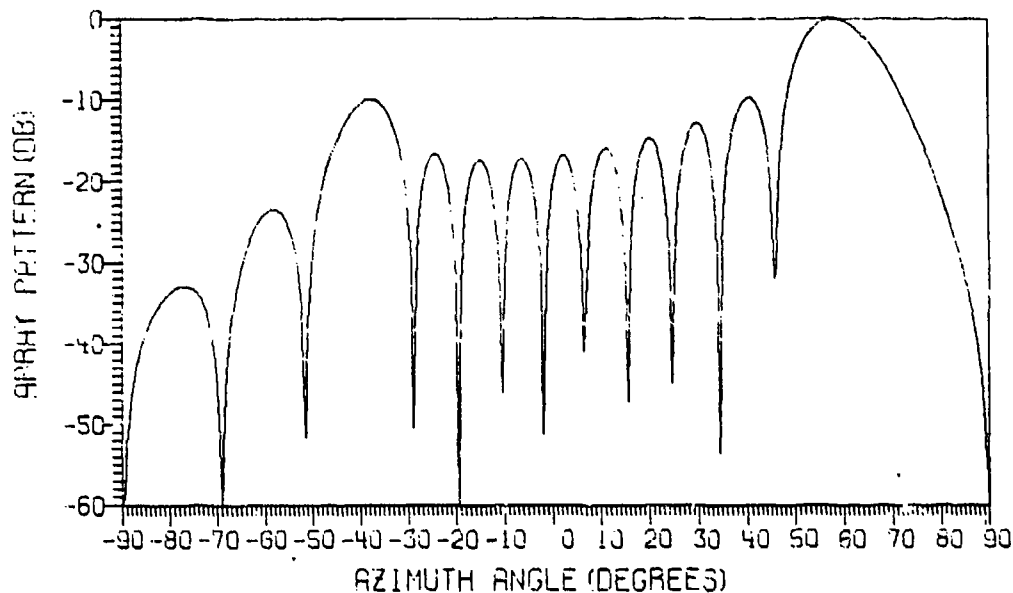and scanned to 30° in azimuth

Fig. 8e — Azimuth pattern of triangular grid (Fig. 6) EATS array located on fuselage
and scanned to 60° in azimuth

Fig. 9a — Elevation pattern of triangular grid (Fig. 7) EATS array located on fuselage

Fig. 9b — Elevation pattern of triangular grid (Fig. 7) EATS array located on fuselage
and scanned to 15° in elevation

Fig. 9c — Azimuth pattern of triangular grid (Fig. 7) EATS array located on fuselage

Fig. 9d — Azimuth pattern of triangular grid (Fig. 7) EATS array located on fuselage
and scanned to 30° in azimuth

15

Fig. 9e — Azimuth pattern of triangular grid (Fig. 7) EATS array located on fuselage
and scanned to 60° in azimuth

To our knowledge, there is no known method of finding optimum spacings, in a
triangular grid array on a circular cylinder, that can be scanned over a given scan range
with no grating lobes or high side lobes. The man-hour limitations on this project did
not allow us to do an extensive investigation in this area. Therefore, it was decided to
approach the problem differently by decreasing the interelement spacing to about 0.5λ
and using the rectangular grid. Also, use of the rectangular grid configuration, makes
it easier to apply the approximate phasing technique, which is discussed earlier in this
report. To obtain interelement spacing of about 0.5λ, the number of elements in the
array are increased from 5×10 to 7×13 with no change in array physical size. In the
remaining discussions, the EATS array is assumed to contain 7×13 elements.

7 × 13 Elements Array

Uniformly spaced array with exact phasing -- Radiation patterns are obtained for
a uniformly spaced 7 × 13 elements EATS array using exact phasing. The results are
shown in Figs. 10a through 10e. When compared to Figs. 5a and 5b, the side lobes
are lower in Figs. 10a and 10b and have no grating lobes in azimuth patterns when
scanned up to 60° in azimuth, as shown in Figures 10c through 10e.

Projected uniformly spaced array with exact phasing — The array elements are dis-
tributed on the curved surface of the circular cylinder so that when projected onto a
plane they have uniform spacing, as discussed earlier in this report Assuming such pro-
jected uniform spacing for the array elements, the required exact steering phases are
supplied to scan the antenna beam. The results are presented in Figs. 11a through 11e.
Figures 11a and 11b show the elevation patterns for 0° and 15° elevation scan angles.

16

The azimuth patterns, for different azimuth scan angles, are shown in Figs. 11c through 11e. These patterns are very similar to the patterns in Figs. 10a through 10e, which are obtained by assuming uniform spacing and exact phasing. This is because the EATS array occupies a smaller arc around the cylinder, and consequently the uniform and projected uniform spacings are very close to each other. The patterns shown in Figs. 11a through 11e will be used later to compare the patterns obtained by using approximate phasing (row-column steering).
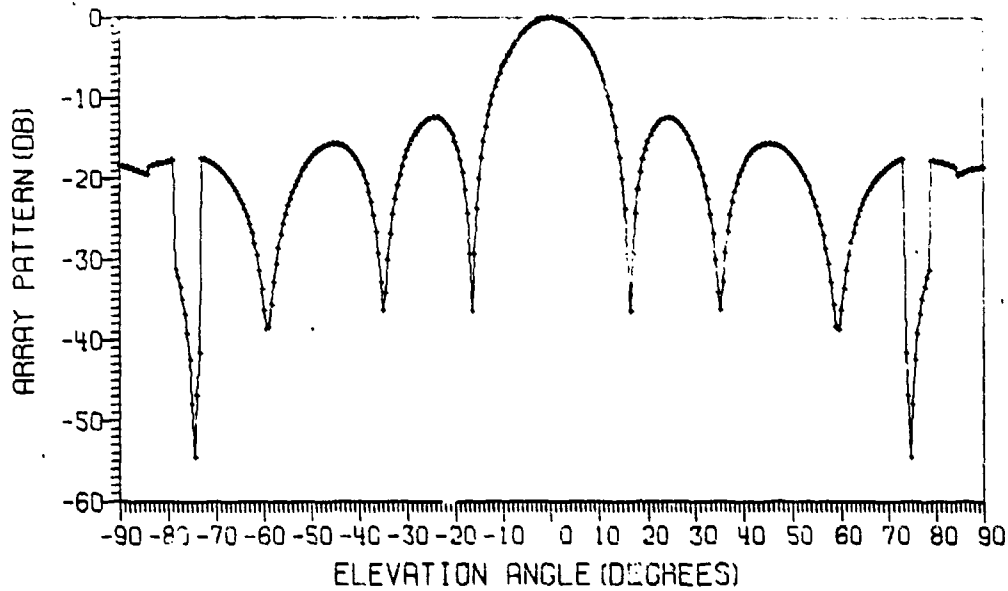
Fig. 10a — Elevation pattern of 7 X 13 EATS array, uniformly spaced on fuselage
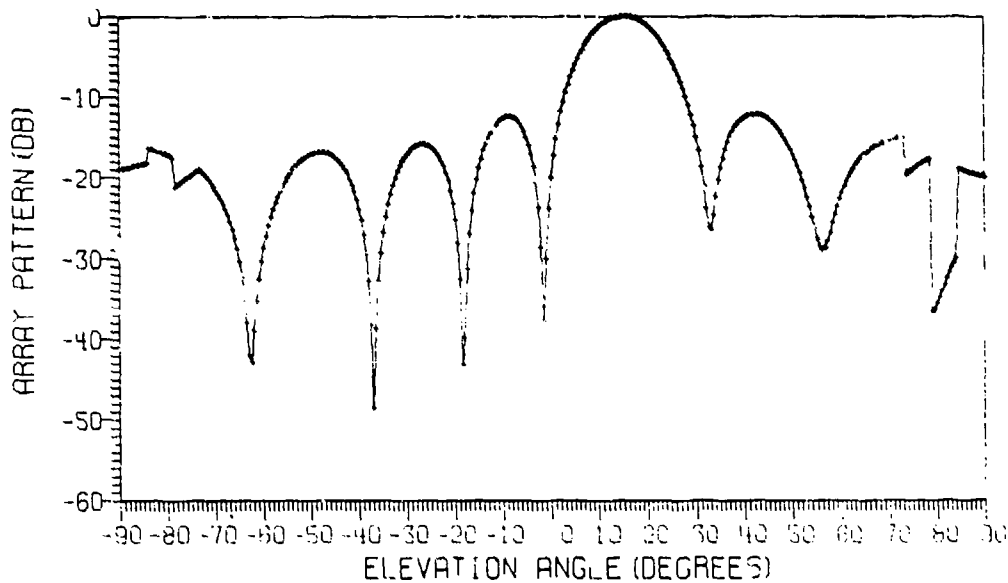
Fig. 10b — Elevation pattern of 7 X 13 EATS array, uniformly spaced on fuselage and scanned to 15° in elevation

17
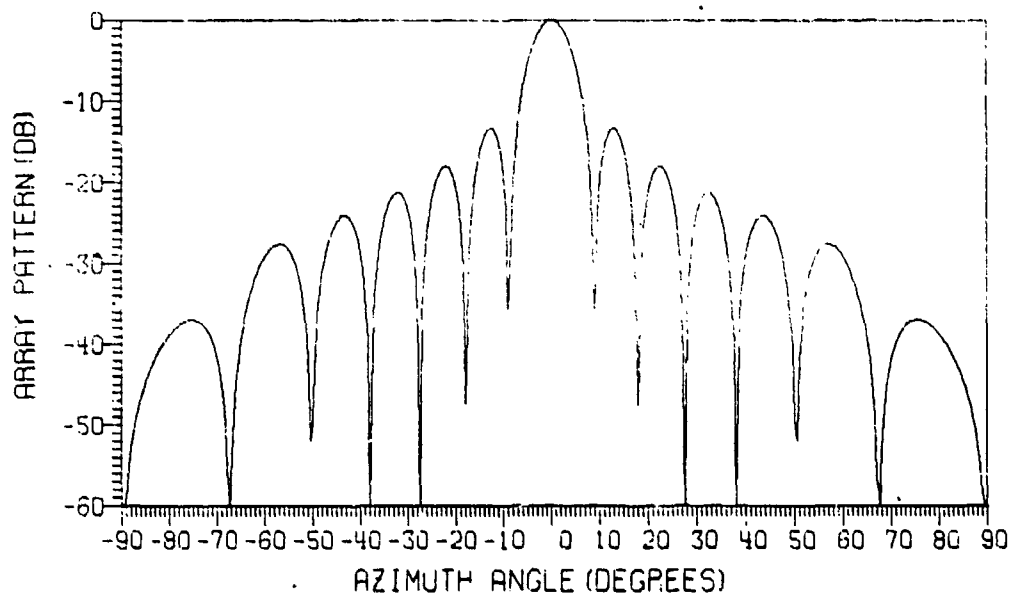
Fig. 10c — Azimuth pattern of 7 X 13 EATS array, uniformly spaced on fuselage
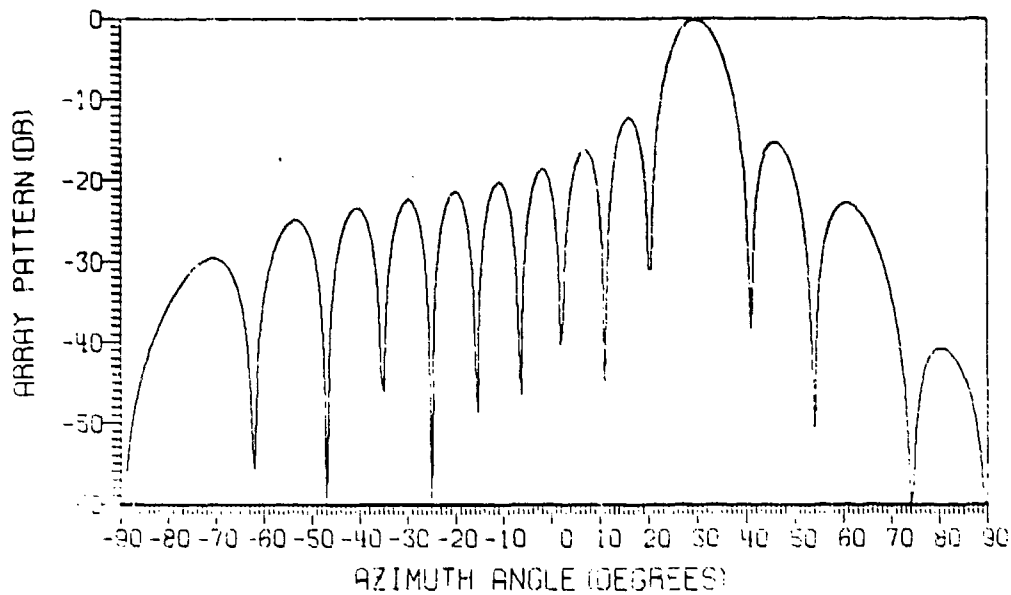
Fig. 10d — Azimuth pattern of 7 X 13 EATS array, uniformly spaced on fuselage
and scanned to 30° in azimuth
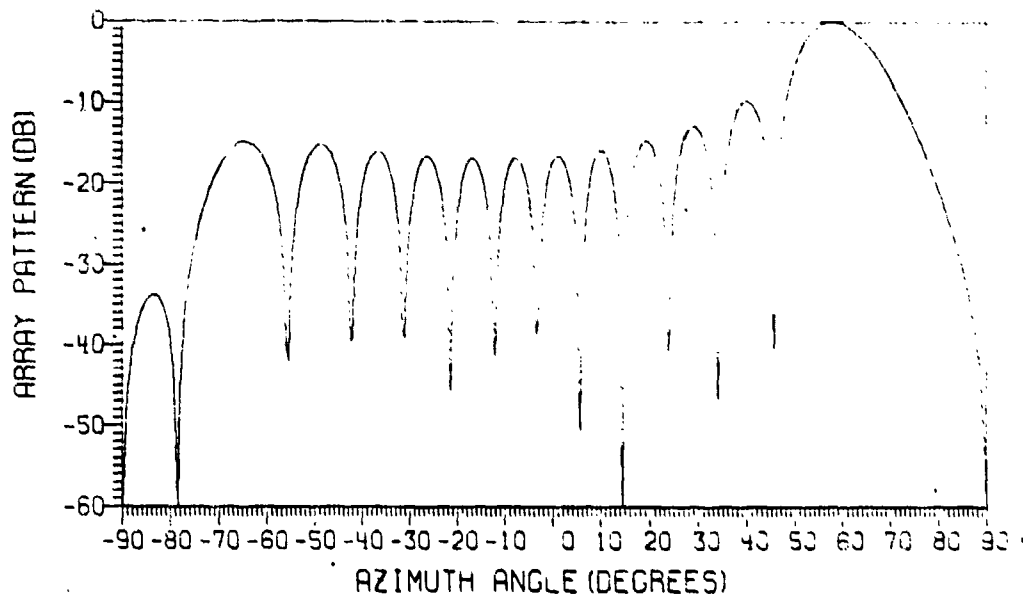
Fig. 10e — Azimuth pattern of 7 X 13 EATS array, uniformly spaced on fuselage
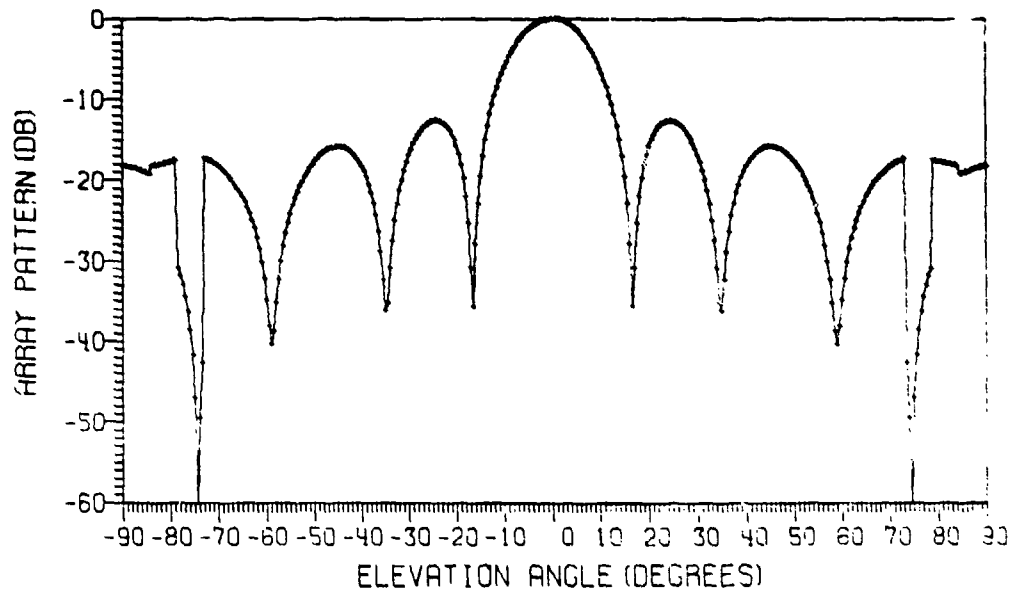and scanned to 60° in azimuth

Fig. 11a — Elevation pattern of 7 X 13 EATS array, projected uniformly spaced on fuselage
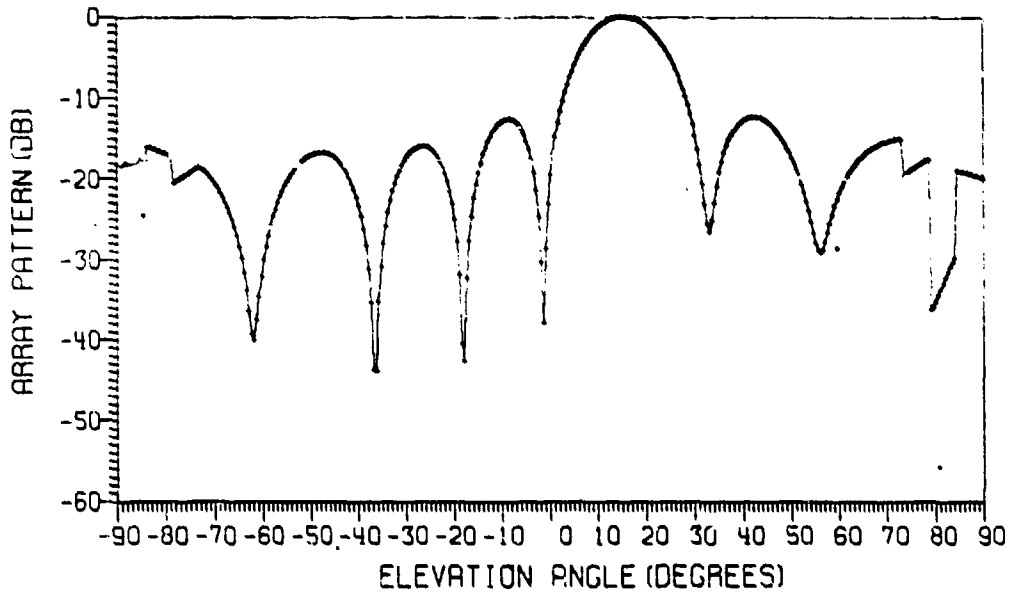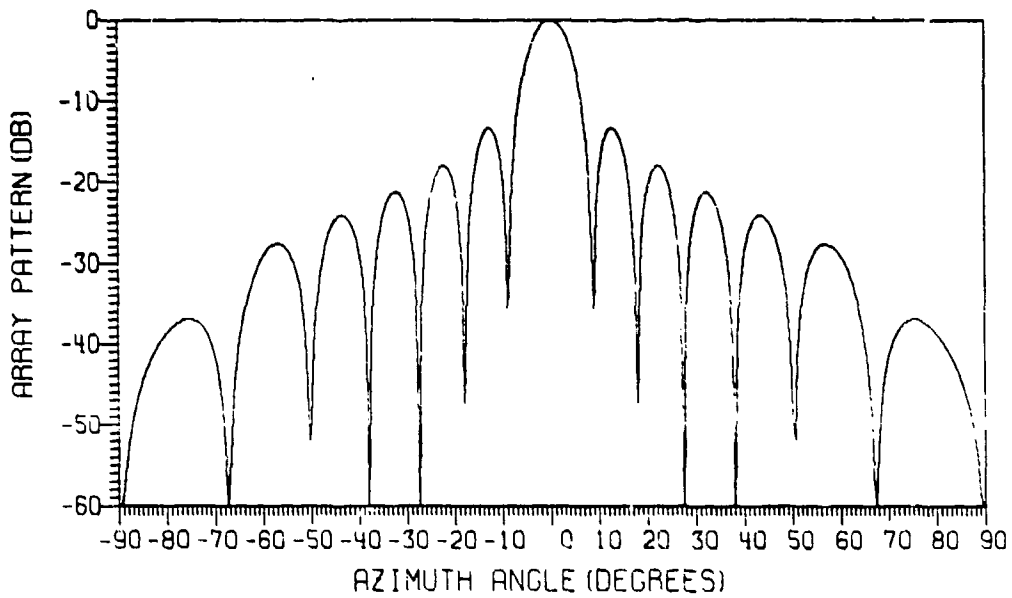
Fig. 11b — Elevation pattern of 7 X 13 EATS array, projected uniformly spaced on fuselage and scanned to 15° in elevation using exact steering phase

Fig. 11c — Azimuth pattern of 7 X 13 EATS array, projected uniformly spaced on fuselage
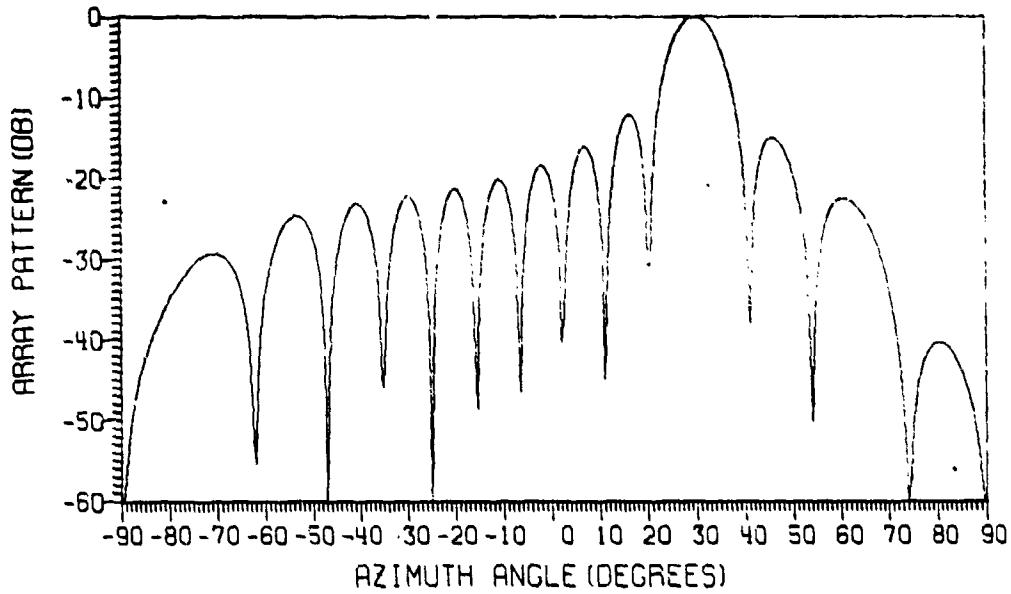
Fig. 11d — Azimuth pattern of 7 X 13 EATS array, projected uniformly spaced on fuselage and scanned to 30° in azimuth using exact steering phase
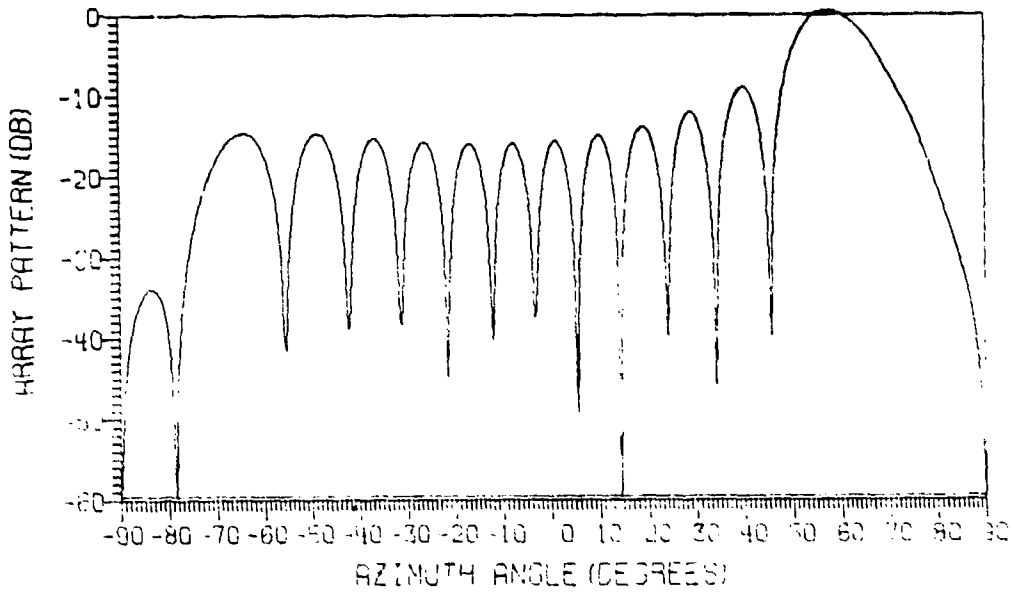

Fig. 11e — Azimuth pattern of 7 X 13 EATS array, projected uniformly spaced on fuselage and scanned to 60° in azimuth using exact steering phase

· *Projected uniformly spaced array with row-column steering* — The element spacing on the curved surface is assumed to be the same as described in the preceding paragraph. However, instead of exact phasing, an approximate phasing is used to scan the beams. The computed radiation patterns are shown in Figs. 12a through 12e. Comparing these patterns with those in Figs. 11a through 11e, we note that the difference between the two sets is very small, and therefore the phase errors introduced by approximate phasing are negligible. This conclusion can also be reached by calculating the phase errors with the equations developed earlier in this report. As discussed earlier, the maximum phase error corresponds to the phase errors in the end elements and when the beam is scanned to the maximum scan range of interest. For EATS array, the end element angular position θ_N from the array broadside is found to be 16.6°, the maximum elevation scan angle θ_S of interest is 15°, and the maximum scan angle φ_S of interest is 60°. Substituting $\theta_N = 16.6°$, $\theta_S = 15°$, and $\varphi_S = 60°$ in Eqs. (2) and (5), we note that the maximum phase error in the end elements is 42° and the maximum rms phase error in the entire EATS array is only 10.5°. This small phase error did not degrade the radiation patterns. However, there is a small loss in gain (0.32 dB) when the beam is scanned to 60° in azimuth, as shown in Table 1. Therefore, it is cost effective to use row-column steering for the EATS array located on the fuselage, with negligible degradation in array performance.

Table 1
EATS Array Characteristics

Array Configuration	Scan Angle		Beamwidth		Relative* Gain (dB)
	Elevation (deg)	Azimuth (deg)	Elevation (deg)	Azimuth (deg)	
Uniformly spaced array of 7 x 13 elements with exact phasing	0	0	14.75	8.0	0
	15	0	15.25	--	0
	0	30	—	9.0	0
	0	60	—	14.0	0
Projected uniformly spaced array of 7 x 13 elements with approximate phasing	0	0	14.75	8.0	0
	15	0	15.25	—	0
	0	30	—	9.0	-0.03
	0	60	—	14.5	-0.32

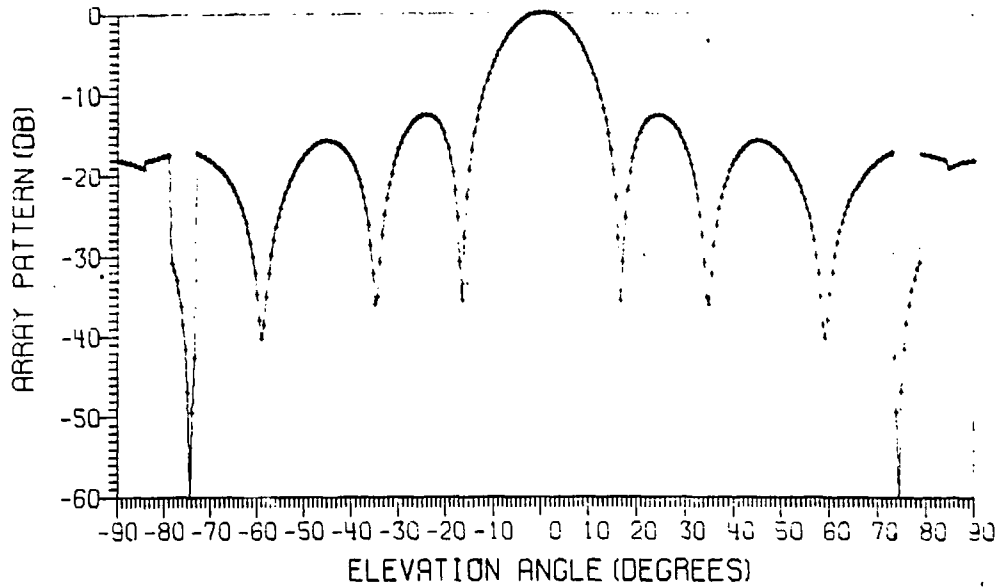*Relative gain with respect to a planar array of the same size.

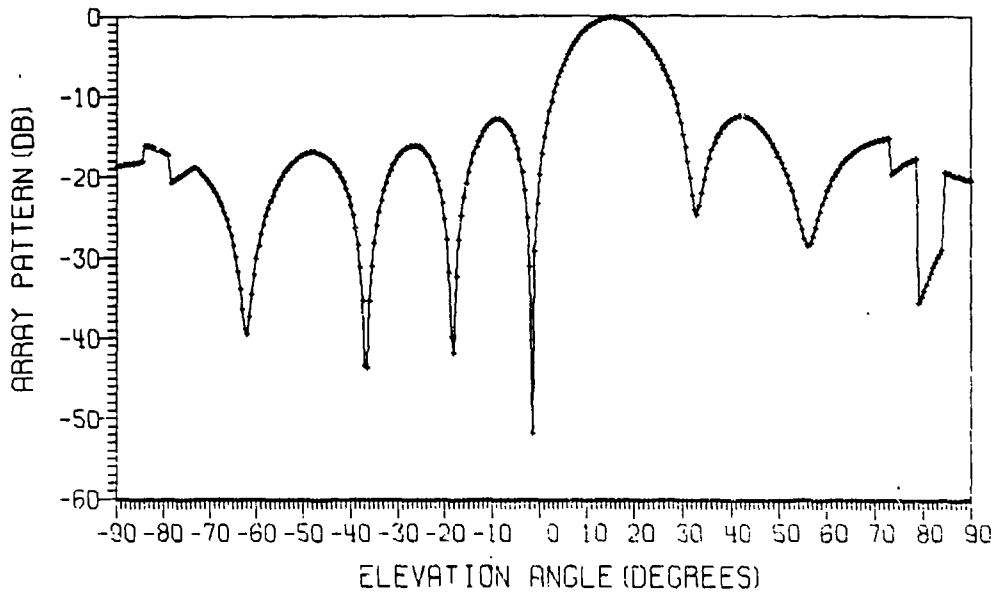Fig. 12a — Elevation pattern of 7 X 13 EATS array, projected uniformly spaced on fuselage

Fig. 12b — Elevation pattern of 7 X 13 EATS array, projected uniformly spaced on fuselage
and scanned to 15° in elevation applying row-column steering

23
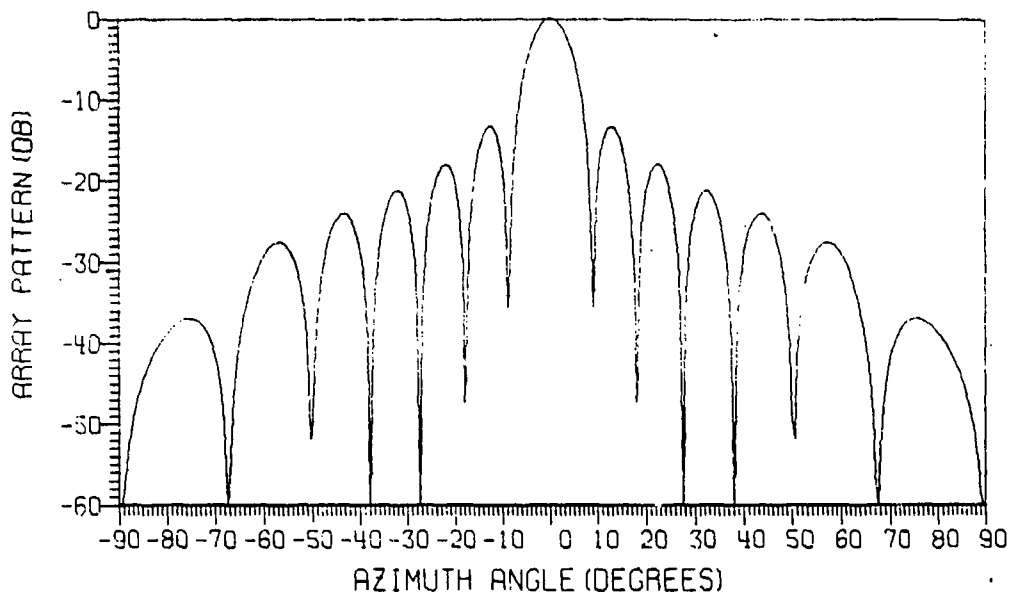
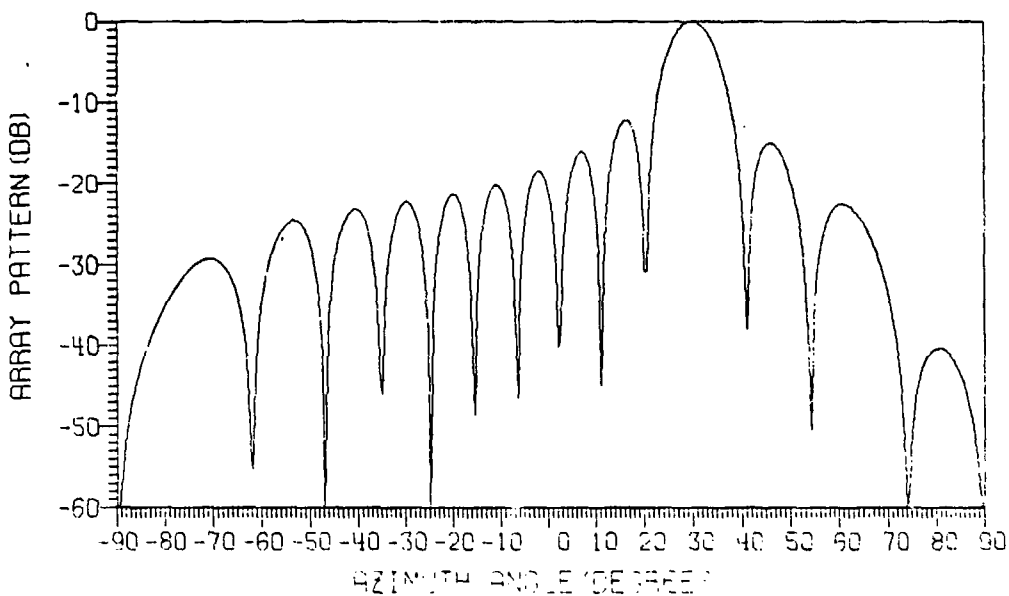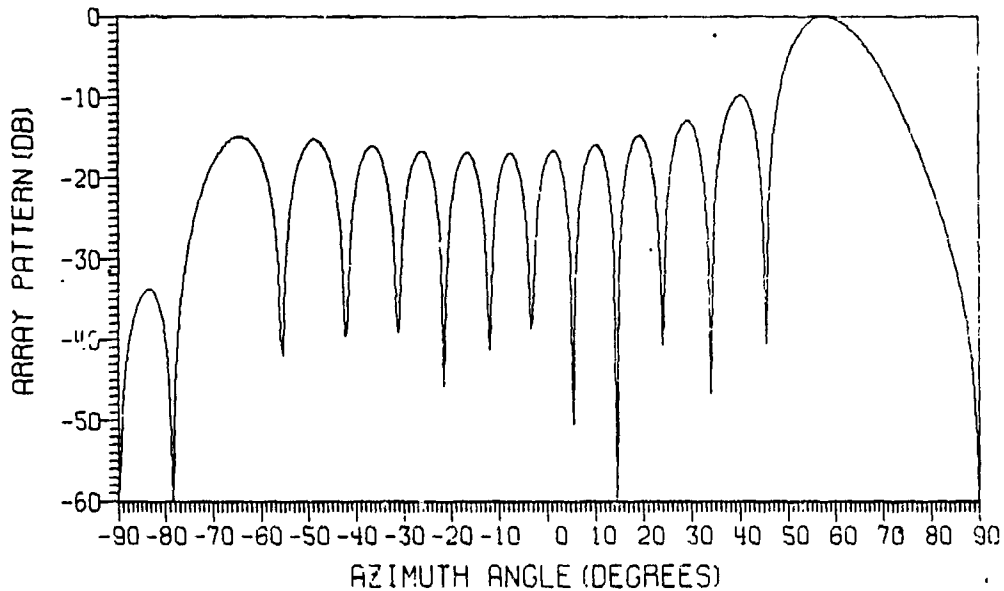Fig. 12c — Azimuth pattern of 7 X13 EATS array, projected uniformly spaced on fuselage

Fig. 12d — Azimuth pattern of 7 X13 EATS array, projected uniformly spaced on fuselage
and scanned to 30° in azimuth applying row-column steering

Fig. 12e — Azimuth pattern of 7 X 13 EATS array, projected uniformly spaced on fuselage
and scanned to 60° in azimuth applying row-column steering

Summary of EATS Array on Fuselage — It is shown that the 5 X 10 element array
proposed in Ref. [2] has undesirable characteristics when placed on the fuselage. The
array performance is improved by increasing the number of elements to 7 X 13 with no
change in array physical size. Finally, it is shown that the array performance did not
degrade by using the familiar planar array, row-column steering which results in substantial
decrease in the cost of hardware implementation. The summary of EATS array character-
istics is given in Table 1. Table 1 shows half-power beamwidths and relative gains for
several scan angles in azimuth and elevation planes. As one would expect, the beamwidth
increases as the beam is scanned away from broadside. As for the gain; theoretically, it
is possible to find the absolute gain of the conformal array by integrating the three-
dimensional array pattern. However, it is difficult, if not impossible, to implement that
procedure even by using a computer. An approximate technique is usually sought in such
cases. For the purpose of this report, the conformal array gain is given as a relative gain
defined as

$$\text{Relative gain} = \frac{\text{Conformal array elements contribution in a given direction}}{\text{Equivalent planar array elements contribution in the same direction}}.$$

The equivalent planar array is assumed to have the aperture equal to the projected aper-
ture of the conformal array and to have the same number of elements. For a planar
array it is well known that the array gain is given by $4\pi A/\lambda^2$, where A is the effective
area and λ is the wavelength. For EATS array the equivalent planar array aperture is
given by $3\lambda \times 6\lambda$, giving a broadside gain of 226 (for 100% efficiency) and the gain
decreases by a factor of $\cos \beta$, as the beam is scanned to an angle β from broadside.
Our computations showed that the gain of EATS conformal array is the same as its

25

equivalent planar array. Therefore, the relative gain column carries 0 dB when exact steering phase is used. When approximate phasing is used, there is a small decrease in gain for EATS array (Table 1). This is because of the small phase errors introduced by the approximate phasing (row-column steering).

TCS Receiving Array

The size of the TCS array is assumed to be 0.7m X 1.4m, as proposed in Ref. [2], which translates to a 10.27λ X 20.54λ array at 4.4 GHz.

16 X 32 Elements Array

A 16 X 32 elements array is proposed in Ref. [2] for TCS. Therefore, it is analyzed first. Assuming that the array elements are uniformly distributed on the fuselage and exact phasing is used to scan the beams, the radiation patterns are obtained for several scan angles in the elevation and azimuth planes; these are shown in Figs. 13a through 13e. From Fig. 13b it is noted that the side lobes increased to high levels when scanned to 15° in elevation. If the required scan angle is increased to 30°, to consider offset configuration, it is conceivable that the side lobes may increase to higher levels. This is mainly due to larger interelement spacing (≈ 0.68λ) in the elevation plane. In Fig. 13e note that the grating lobes appeared when the beam was scanned to 60° in the azimuth plane. This is because of the larger interelement spacing (≈ 0.66λ) in the azimuth plane. A triangular grid structure did not remedy the situation (results for TCS array are not
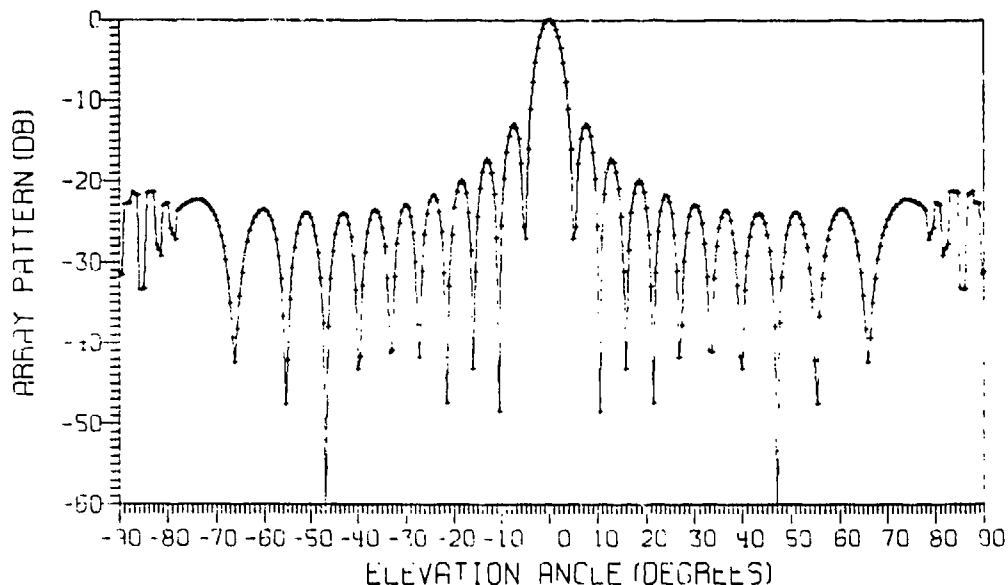

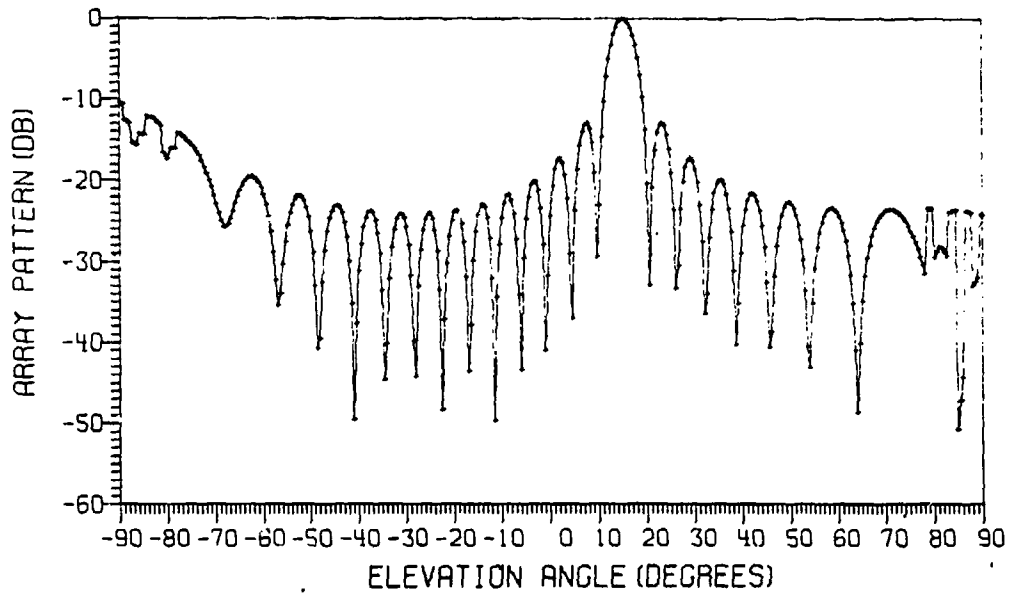Fig. 13a — Elevation pattern of 16 X 32 TCS array, uniformly spaced on fuselage

26

Fig. 13b — Elevation pattern of 16 X 32 TCS array, uniformly spaced on fuselage and scanned to 15° in elevation
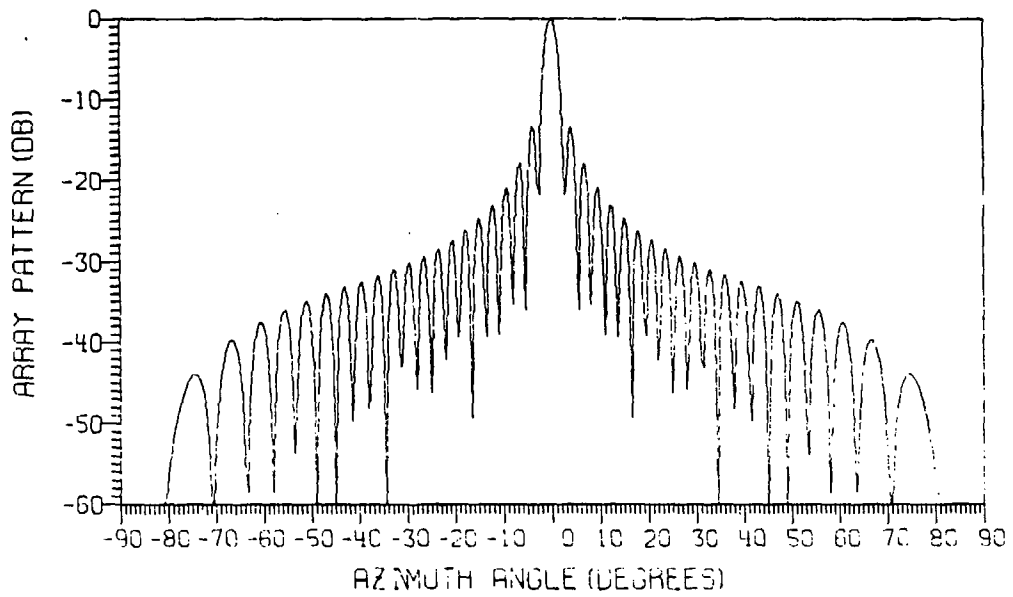
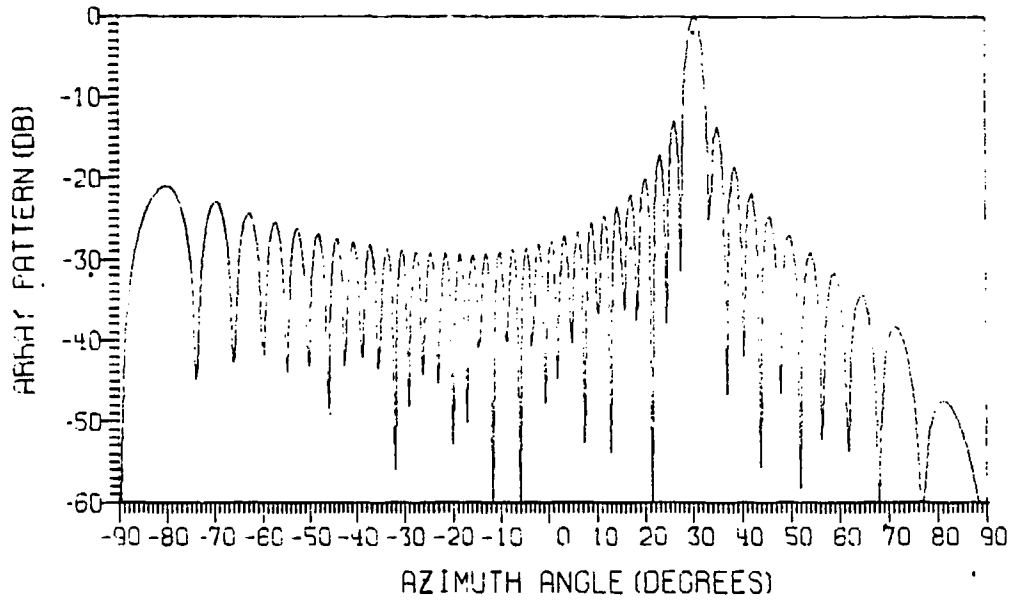Fig. 13c — Azimuth pattern of 16 X 32 TCS array, uniformly spaced on fuselage

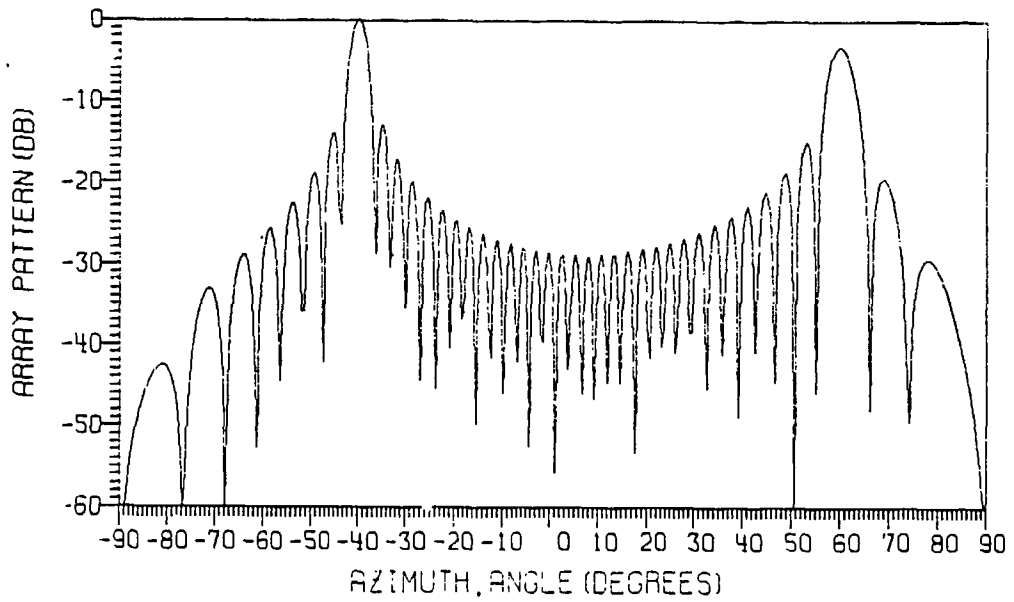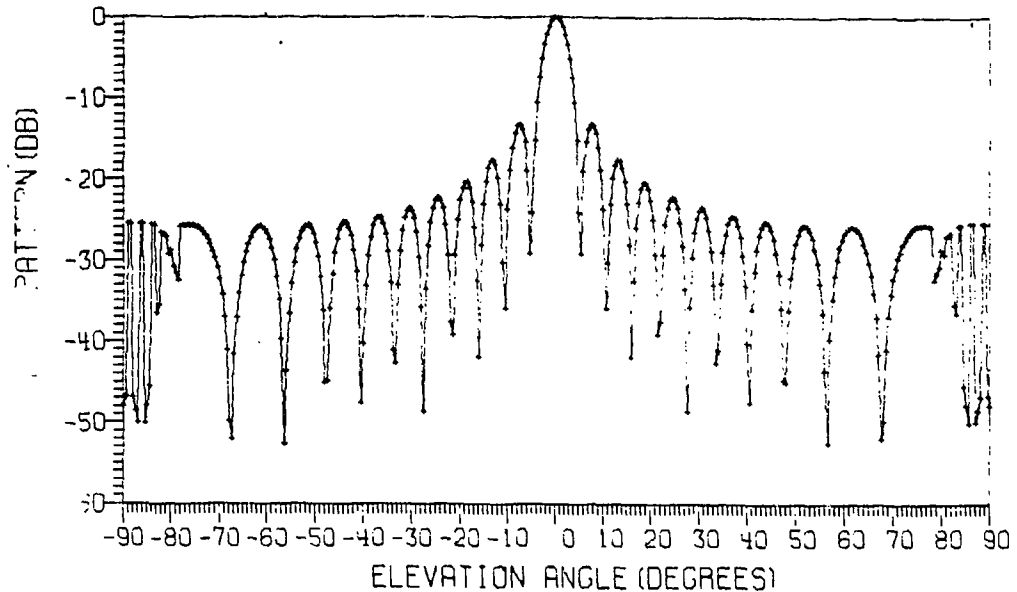Fig. 13d — Azimuth pattern of 16 × 32 TCS array, uniformly spaced on fuselage and scanned to 30° in azimuth

Fig. 13e — Azimuth pattern of 16 × 32 TCS array, uniformly spaced on fuselage and scanned to 60° in azimuth

included because the conclusions are similar to EATS array with triangular grid). Therefore, it was decided to increase the number of elements in the array to 20 X 40 and retain the same physical size so that the interelement spacing is approximately 0.5λ in azimuth and in elevation planes. This will eliminate the undesirable characteristics noted with the 16 X 32 element array.

20 X 40 Element Array

Uniformly spaced array with exact phasing — Radiation patterns were obtained for a 20 X 40 element TCS array with uniform spacing and using exact phasing to scan the beam. The results are shown in Figs. 14a through 14f. When compared to the patterns shown in Figs. 13a through 13e, the side lobes are lower and no grating lobes appeared in the azimuth pattern when scanned up to 60° in azimuth.

Fig. 14a — Elevation pattern of 20 X 40 TCS array, uniformly spaced on fuselage
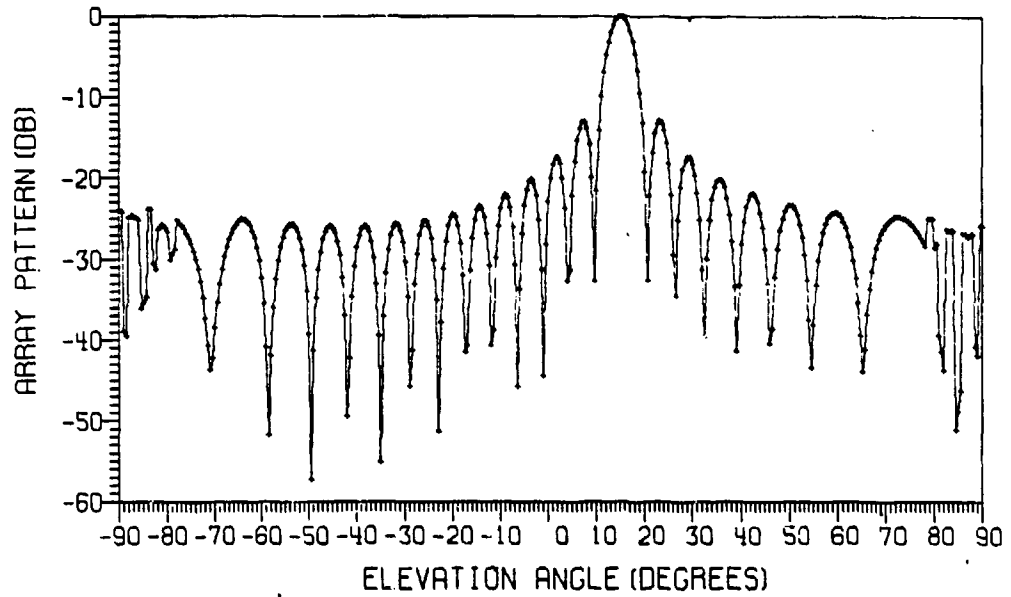
29

Fig. 14b — Elevation pattern of 20 × 40 TCS array, uniformly spaced on fuselage and scanned to 15° in elevation applying exact steering phase
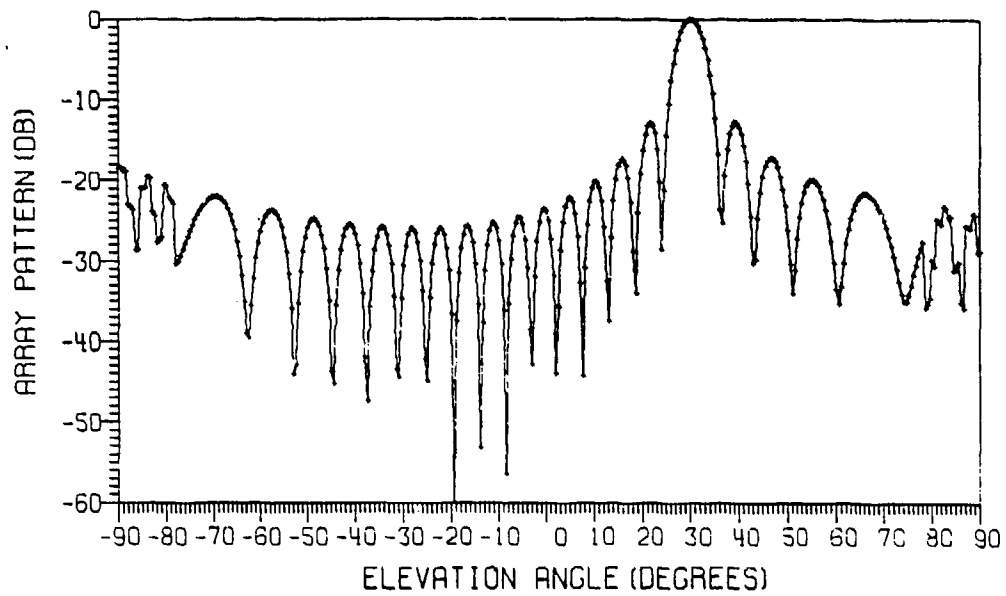

Fig. 14c — Elevation pattern of 20 × 40 TCS array, uniformly spaced on fuselage and scanned to 30° in elevation applying exact steering phase
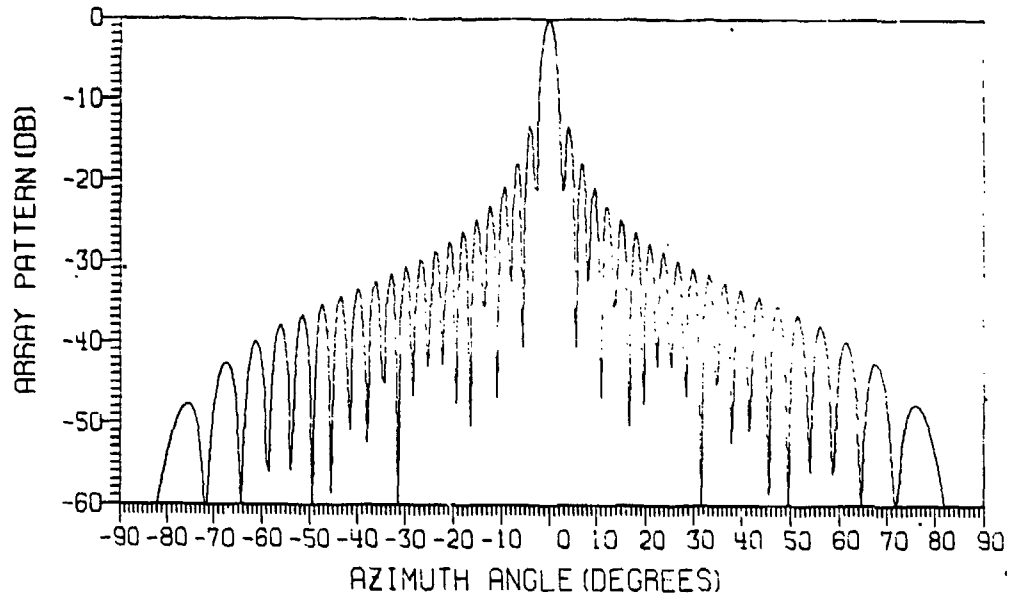
30

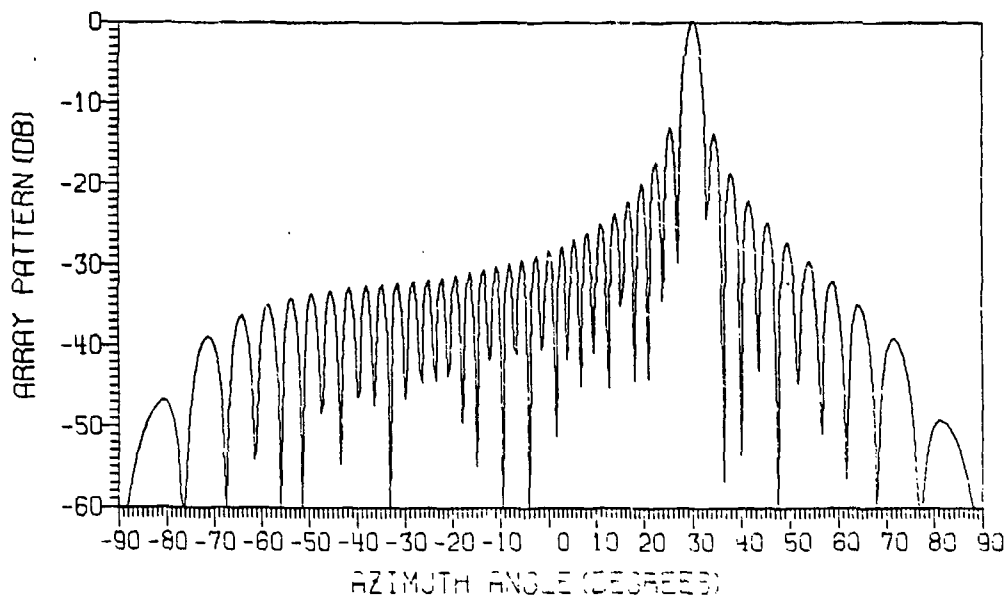Fig. 14d — Azimuth pattern of 20 X 40 TCS array, uniformly spaced on fuselage

Fig. 14e — Azimuth pattern of 20 X 40 TCS array, uniformly spaced on fuselage and scanned to 30° in azimuth applying exact steering phase
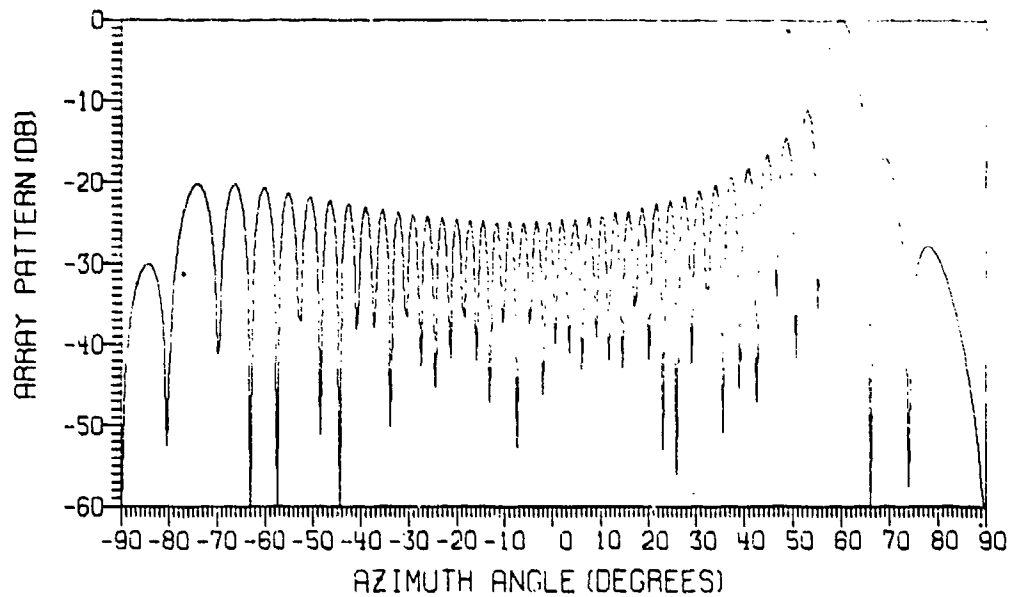
Fig. 14f — Azimuth pattern of 20 X 40 TCS array, uniformly spaced on fuselage and scanned
to 60° in azimuth applying exact steering phase

Projected uniformly spaced array with row-column steering — The array elements
were located on the fuselage so that they have projected uniform spacing, as discussed earlier.
Then, a row-column steering was used to scan the array pattern. The computed results
are shown in Figs. 15a through 15f. Comparing these patterns with those shown in
Figs. 14a through 14f, shows that there is negligible difference. Therefore, for TCS array
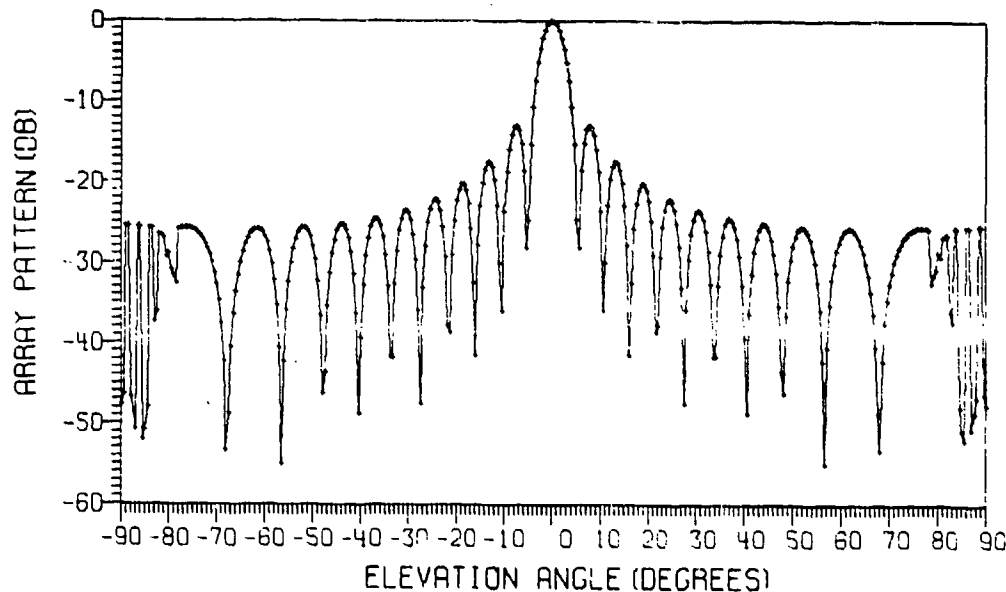

Fig. 15a — Elevation pattern of 20 X 40 TCS array, projected uniformly spaced on fuselage
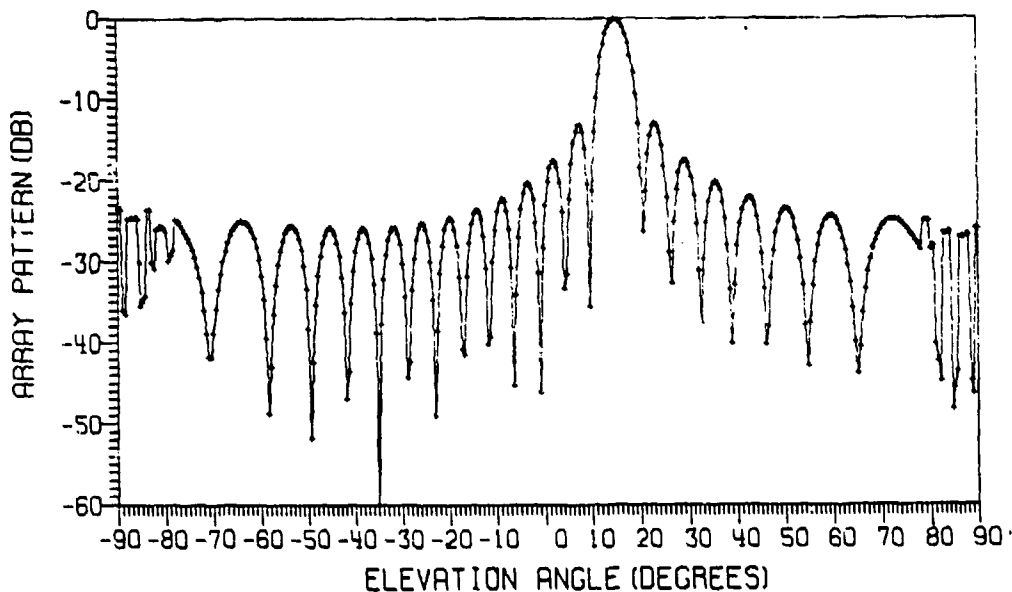
32

Fig. 15b — Elevation pattern of 20 X 40 TCS array, projected uniformly spaced on fuselage
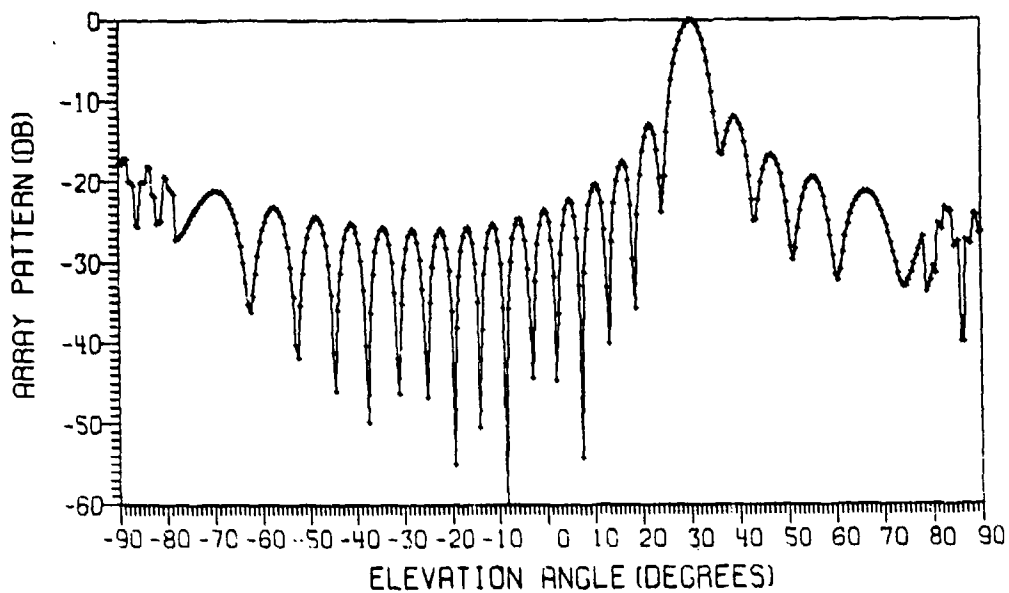and scanned to 15° in azimuth applying row-column steering

Fig. 15c — Elevation pattern of 20 X 40 TCS array, projected uniformly spaced on fuselage
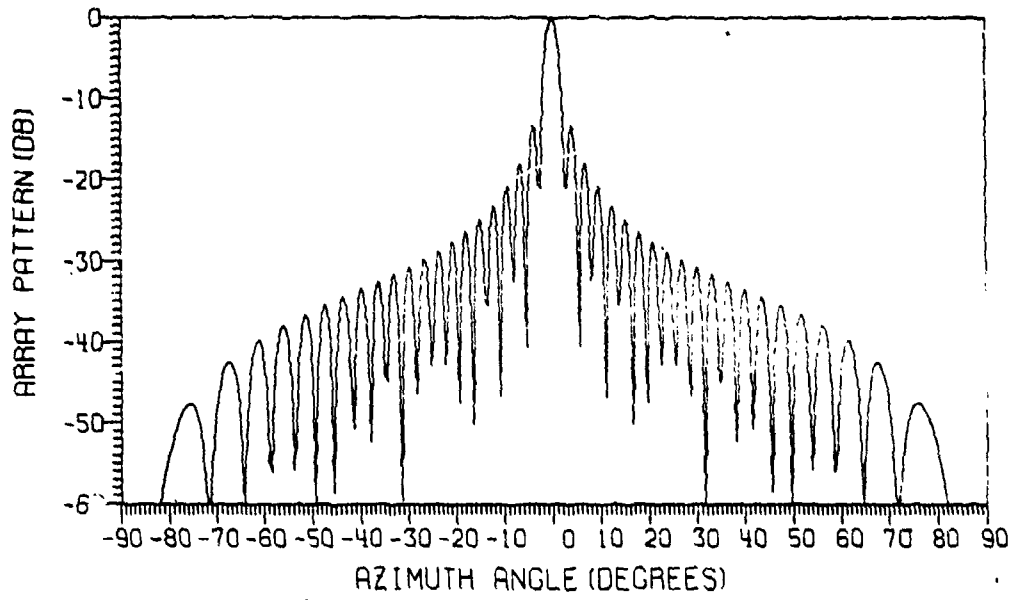and scanned to 30° in elevation applying row-column steering

Fig. 15d — Azimuth pattern of 20 × 40 TCS array, projected uniformly spaced on fuselage
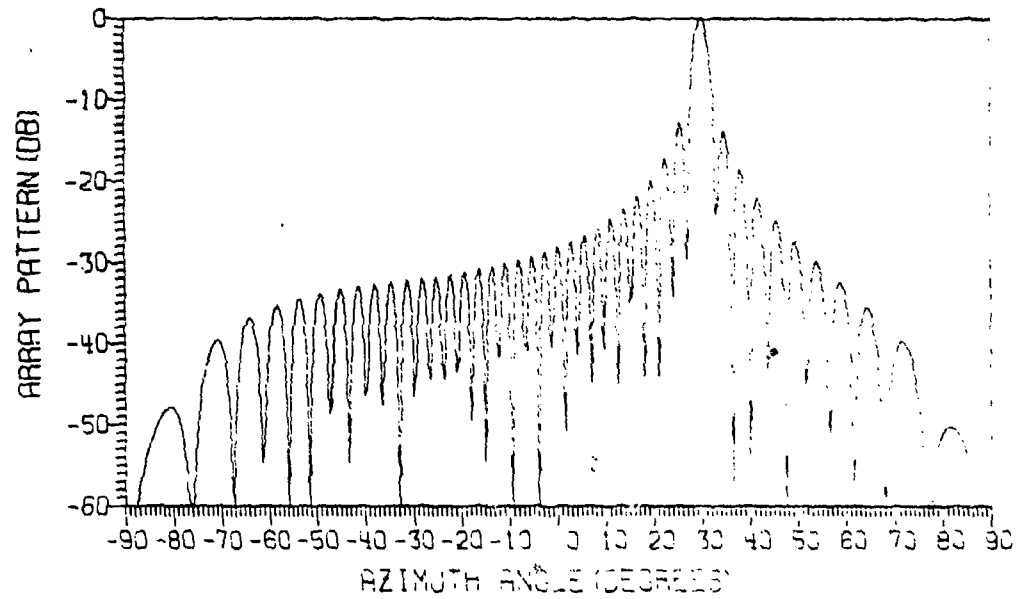

Fig. 15e — Azimuth pattern of 20 × 40 TCS array, projected uniformly spaced on fuselage
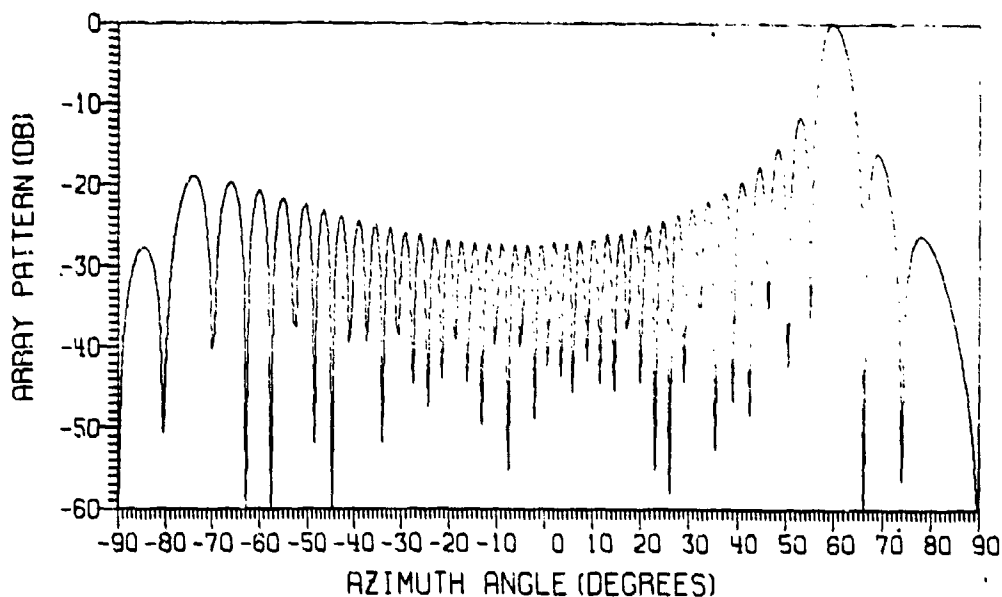and scanned to 30° in azimuth applying row-column steering

Fig. 15f — Azimuth pattern of 20 X 40 TCS array, projected uniformly spaced on fuselage
and scanned to 60° in azimuth applying row-column steering

Table 2
TCS Array Characteristics

Array Configuration	Scan Angle		Beamwidth		Relative* Gain (dB)
	Elevation (deg)	Azimuth (deg)	Elevation (deg)	Azimuth (deg)	
Uniformly spaced array of 20 x 40 elements with exact phasing	0	0	4.75	2.25	0
	15	0	5.0	—	0
	0	30	—	2.75	0
	0	60	—	4.75	0
Projected uniformly spaced array of 20 x 40 elements with planar array phasing	0	0	4.75	2.25	0
	15	0	5.0	—	0
	0	30	—	2.75	-0.1
	0	60	—	4.9	-1.25

*Relative gain with respect to a planar array of the same size.

on the fuselage, it is cost effective to use approximate phasing with negligible degradation in array patterns. Note, however, that the phase errors introduced some loss in gain, as shown in Table 2, especially when the beam was scanned to 60° in azimuth. For this maximum scan range, it can be shown using Eqs. (2) and (5) that the maximum phase error in the end element is 103°. However, the maximum rms phase error in TCS array is only 26°. These phase errors result in a small gain loss as the beam is scanned to 60° in azimuth.

Summary of TCS array on fuselage — The 16 X 32 element array proposed in Ref. [2] for TCS gives undesirable characteristics when placed on the fuselage of P-3 aircraft. The array performance is improved by increasing the number of elements to 20 X 40 with no change in array physical size. It is shown that using row-column steering did not degrade the array pattern, but there is a small loss in gain, especially when the beam is scanned to 60° in azimuth. Therefore, it is suggested that the approximate phasing could be used for TCS array. The array characteristics are summarized in Table 2.

TMS Array

The array proposed in Ref. [2] for TMS is electrically and physically small. Therefore, its performance characteristics can be expected to be similar to that of the EATS and TCS arrays. In addition, a larger TMS array may be needed in the actual implementation. It was therefore decided to study only the characteristics of larger TMS arrays. Because the computation time for obtaining radiation patterns of a large conformal array becomes too excessive, and because the radiation pattern of an array on a circular cylinder can be approximated by the product of the azimuth and elevation patterns, it was decided to study only the elevation patterns when the array is placed around a circular cylinder. The azimuth patterns are similar to those of a large planar array. In what follows, the results of two arrays with different sizes will be discussed.

Circular Arc Array with 32 Elements — The aperture of the 32-element array was chosen such that the aperture of the circular arc array projected onto a line, as explained earlier, is 15.5λ (6.9 ft for f = 2.2 GHz) so that the average projected interelement spacing is 0.5λ. For P-3 aircraft fuselage, this will translate into a circular arc array length of 16.7λ and the arc angle of 75.6°.

Uniformly spaced array with exact phasing — When the 32 elements are distributed uniformly on the circular arc, the interelement spacing is ≈ 0.54λ. The radiation patterns for this uniform array are shown in Figs. 16a through 16c for 0°, 15°, and 30° elevation scan angles. The beam scanning is accomplished by applying the required exact steering phases. These patterns will be used to compare and judge the performance of the projected uniformly spaced arrays.
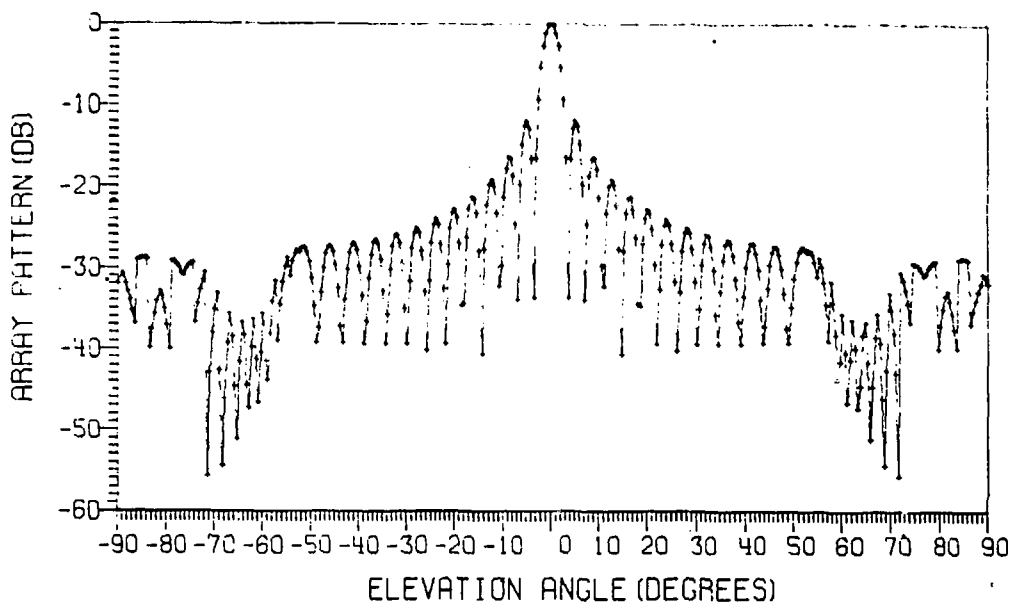
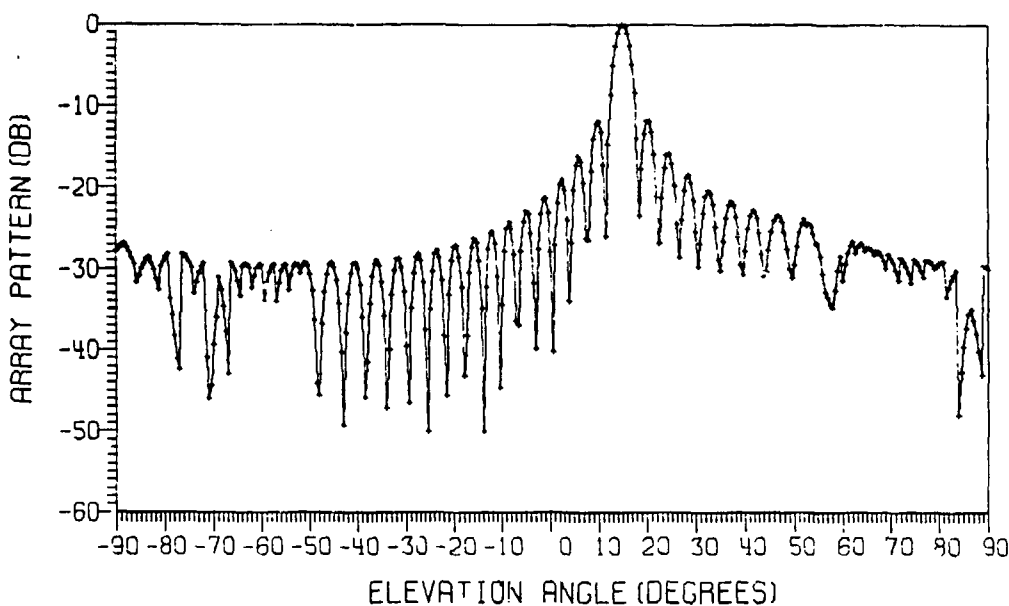Fig. 16a — Elevation pattern of 32 X 1 TMS array, uniformly spaced around fuselage

Fig. 16b — Elevation pattern of 32 X 1 TMS array, uniformly spaced around fuselage
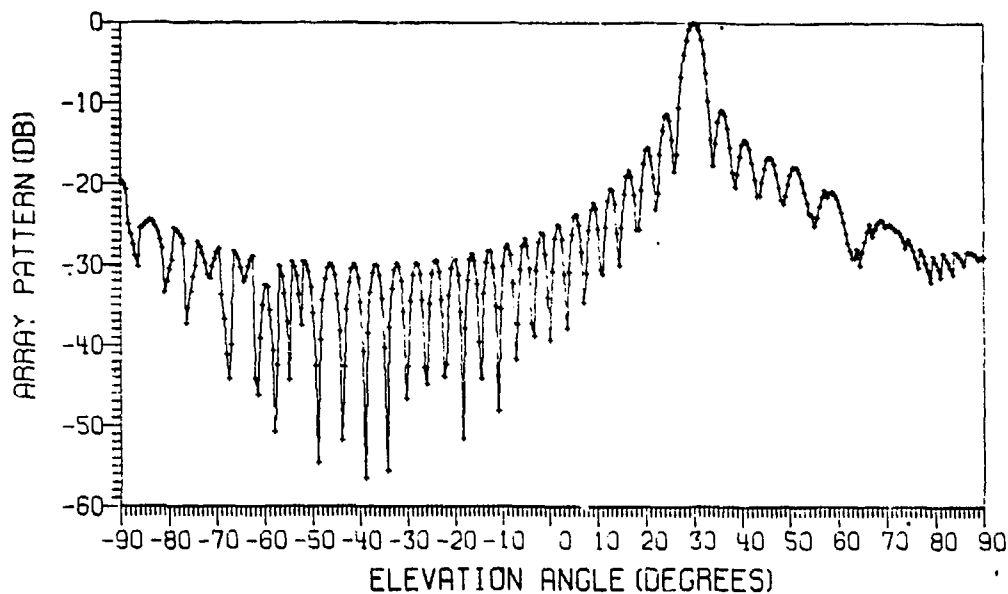and scanned to 15° in elevation applying exact steering phase

Fig. 16c — Elevation pattern of 32 X 1 TMS array, uniformly spaced around fuselage
and scanned to 30° in elevation applying exact steering phase

Projected uniformly spaced array with exact phasing — The array elements are
distributed on the circular arc in such a way that they have equal projected interelement
spacing. By knowing the element locations on the circular arc, one could find the
exact steering phase required to scan the beam. The computed results are shown in
Figs. 17a through 17c. When these are compared with the patterns of uniformly spaced
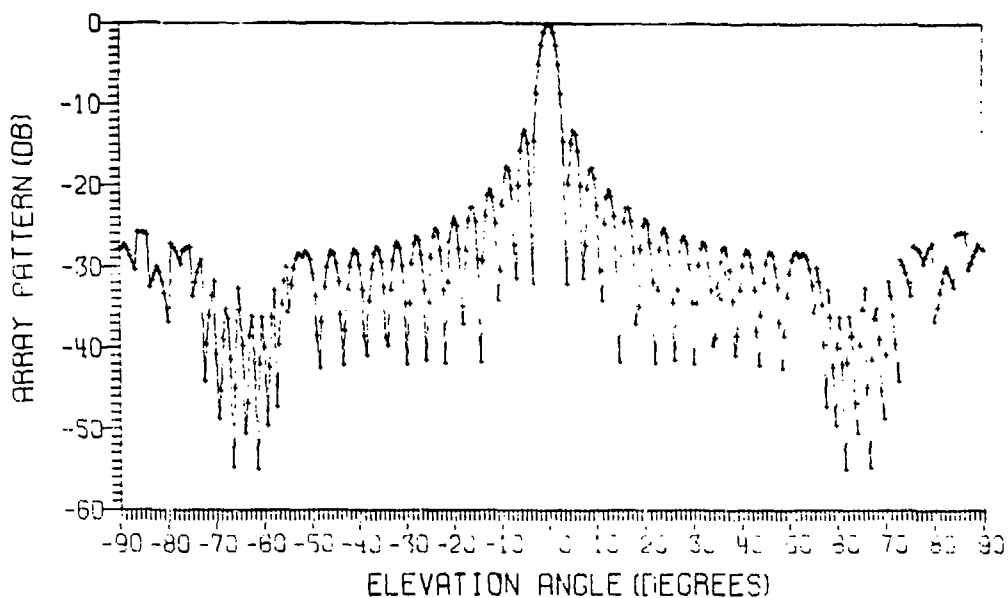arrays shown in Figs. 16a through 16c, the patterns are seen to be similar except that

Fig. 17a — Elevation pattern of 32 X 1 TMS array, projected uniformly spaced around fuselage
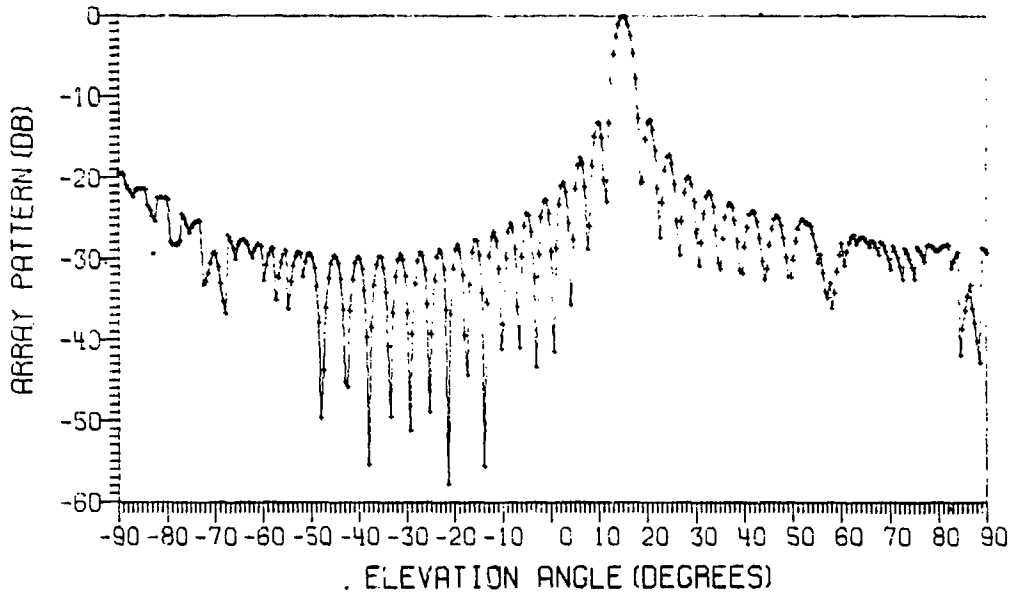
38

Fig. 17b — Elevation pattern of 32 × 1 TMS array, projected uniformly spaced around fuselage and scanned to 15° in elevation applying ? exact steering phase
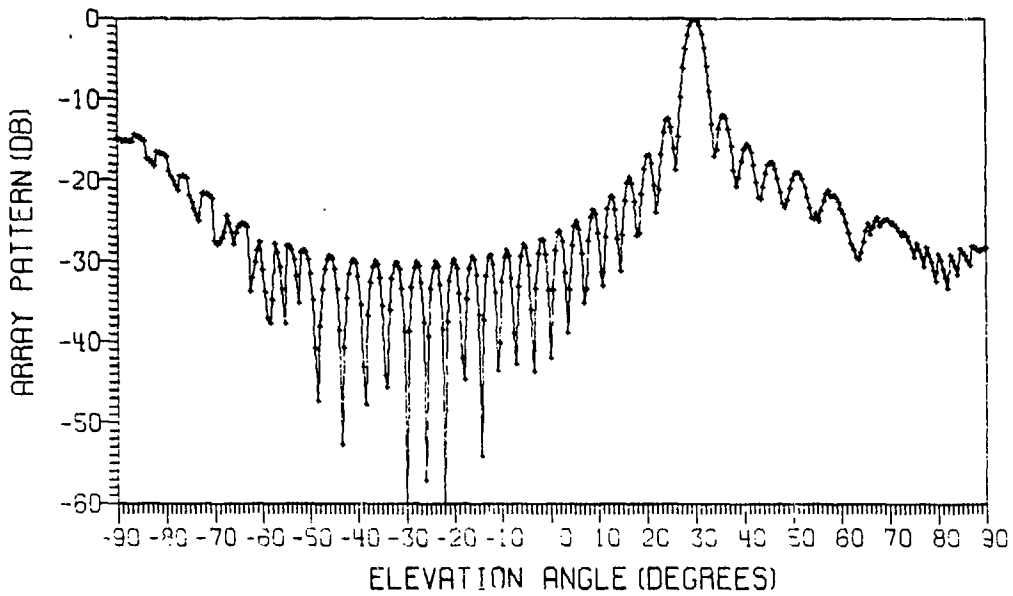

Fig. 17c — Elevation pattern of 32 × 1 TMS array, projected uniformly spaced around fuselage and scanned to 30° in elevation applying exact steering phase

the faraway side lobes increased as the beam was scanned for projected uniform array. This is caused by the larger interelement spacing near the aperture end of the projected uniformly spaced arc array. The patterns shown in Figs. 17a through 17c will be used to compare with the radiation patterns of a projected uniformly spaced array with row-column steering. This will show the effect of approximate phasing more clearly for larger conformal arrays.

Projected uniformly spaced array with linear array phasing — For this, the element distribution is assumed to be the same as stated in the preceding paragraph. However, instead of exact phasing, an approximate phasing is used to scan the beams. The corresponding radiation patterns for elevation scan angles of 0°, 15°, and 30° are shown in Figs. 18a through 18c. Comparing these with the patterns of Figs. 17a through 17c, indicates that up to 15° scan the two approaches give similar patterns. However, as the scan angle is increased to 30°, the pattern obtained by approximate phasing (Fig. 18c) is degraded with increased beamwidth, decreased gain, increased side lobes, and a broad shoulder formation. Therefore, it may be concluded that for a 32-element arc array the approximate phasing could be used for ±15° scanning range with negligible degradation in array performance. For larger scan range, this simplification may not be possible.

Circular Arc Array with 48 Elements — The aperture of the 48-element array was chosen such that the projected aperture length is 23.5λ (10.55 ft at 2.2 GHz), so that the average projected interelement spacing is 0.5λ. For P-3 aircraft fuselage this will translate into a circular array with arc length of 30.25λ and the arc angle of 137°.
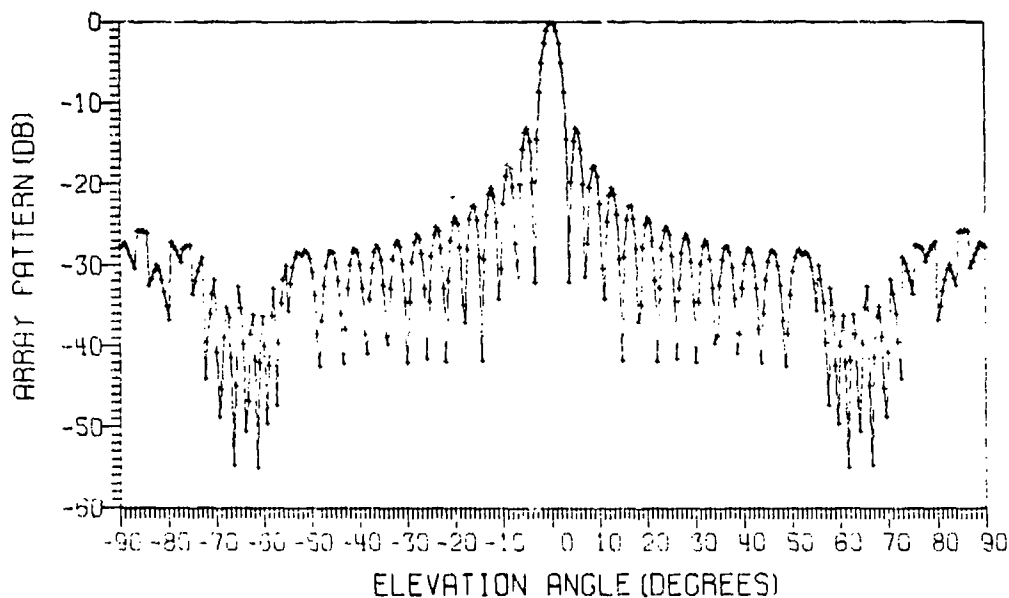

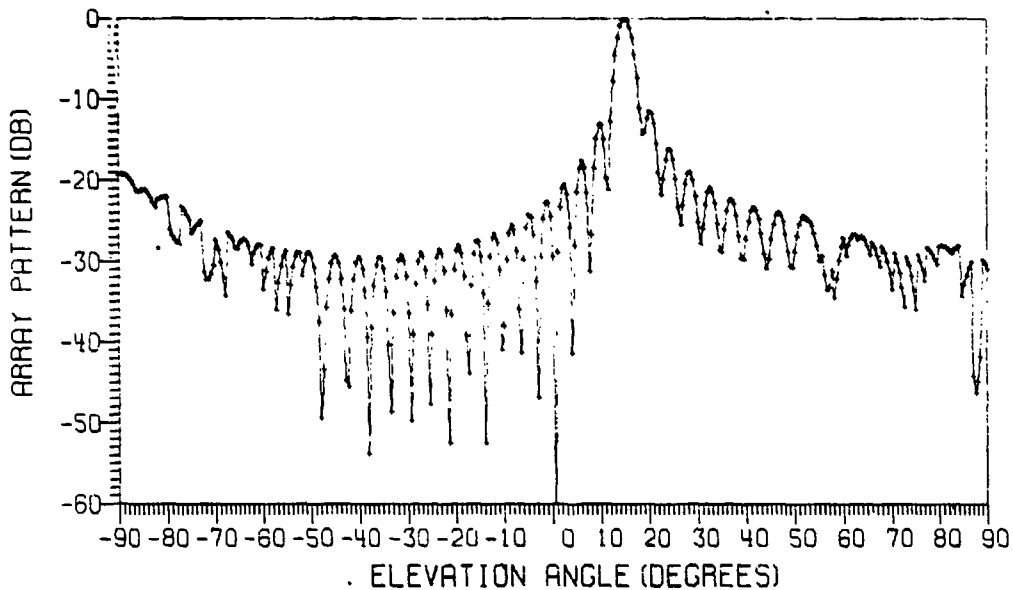Fig. 18a — Elevation pattern of 32 X 1 TMS array, projected uniformly spaced around fuselage

Fig. 18b — Elevation pattern of 32 X 1 TMS array, projected uniformly spaced around fuselage
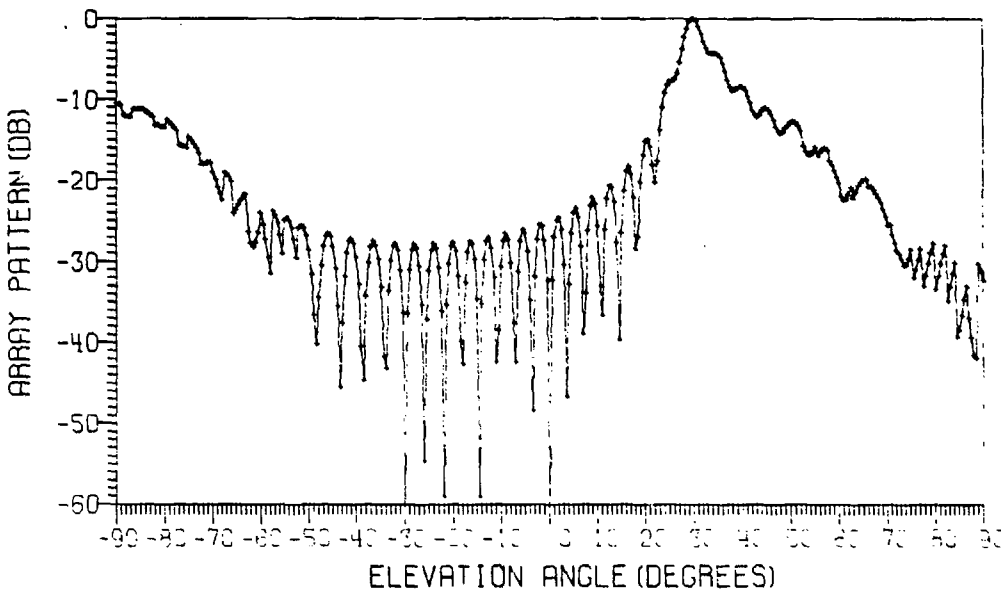and scanned to 15° in elevation applying linear array phasing

Fig. 18c — Elevation pattern of 32 X 1 TMS array, projected uniformly spaced around fuselage
and scanned to 30° in e'evation applying linear array phasing

Uniformly spaced array with exact phasing — When the 48 elements are distributed uniformly on the circular arc, the interelement spacing is ≈ 0.63λ. The computed radiation patterns for this uniform array are shown in Figs. 19a through 19c for different elevation scan angles. The beam scanning was accomplished by applying the required exact steering phases. From Figs. 19b and 19c we see that the grating lobes appeared when the beams were scanned to 15° and 30°, respectively. This is due to the larger interelement spacing (0.63λ). To eliminate these grating lobes the interelement spacing should be decreased by increasing the number of array elements if the aperture size is to remain the same. However, we will show in the next section that the grating lobes can be eliminated by projected uniform element distribution with no increase in the number of elements.
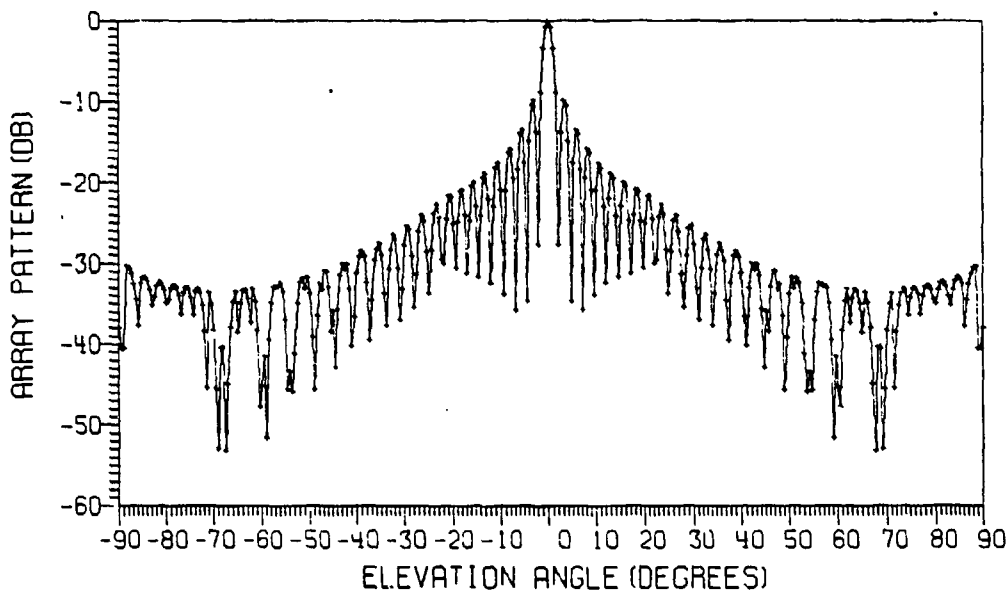

Fig. 19a — Elevation pattern of 48 × 1 TMS array, uniformly spaced around fuselage
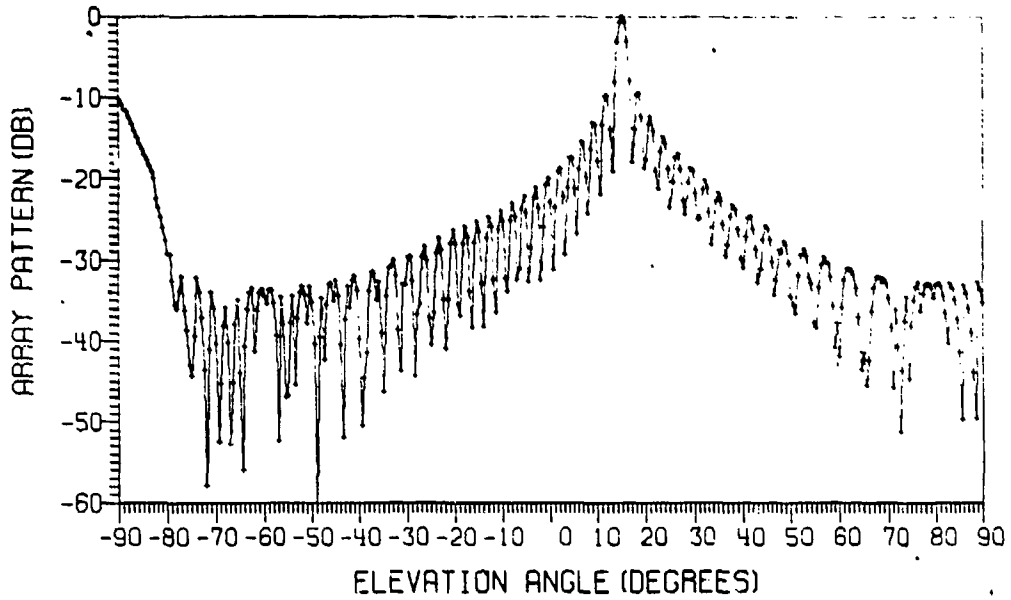
Fig. 19b — Elevation pattern of 48 X 1 TMS array, uniformly spaced around fuselage
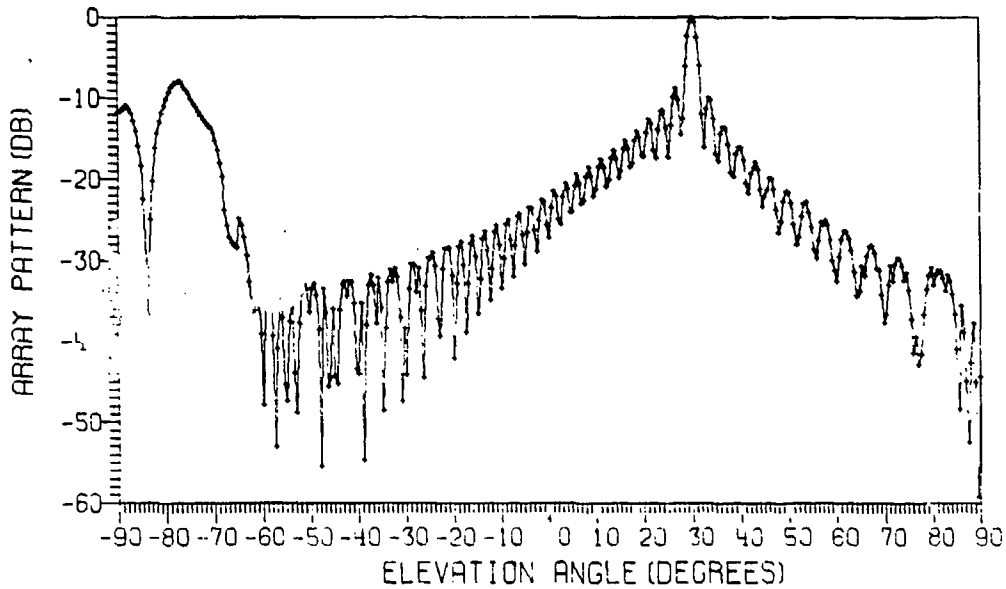and scanned to 15° in elevation applying exact steering phase

Fig. 19c — Elevation pattern of 48 TMS array, uniformly spaced around fuselage
and scanned to 20 in elevation applying exact steering phase

Projected uniformly spaced array with exact phasing — The array elements were
distributed on the circular arc so that they had equal projected interelement spacing.
By knowing the element location on the circular arc, one could apply the exact steering
phase required to scan the beam. The computed patterns are shown in Figs. 20a through
20c. A comparison with the patterns of the uniformly spaced array shown in Figs. 19a
through 19c shows that the main-beam regions are quite similar and that the grating
lobes are suppressed for a projected uniform array. The effect of using approximate
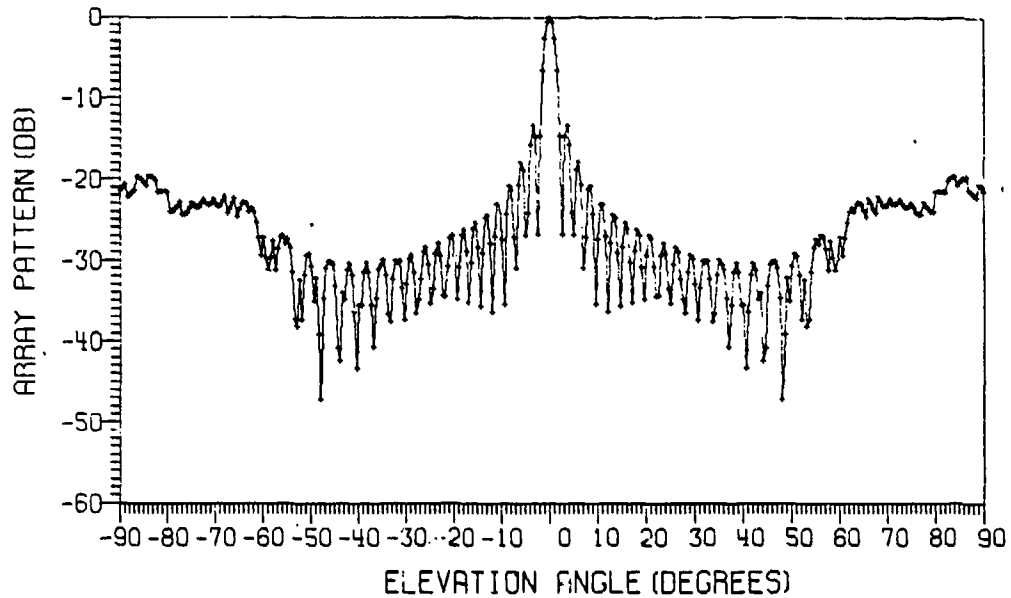phasing will be discussed next.

Fig. 20a — Elevation pattern of 48 X 1 TMS array, projected uniformly spaced around fuselage
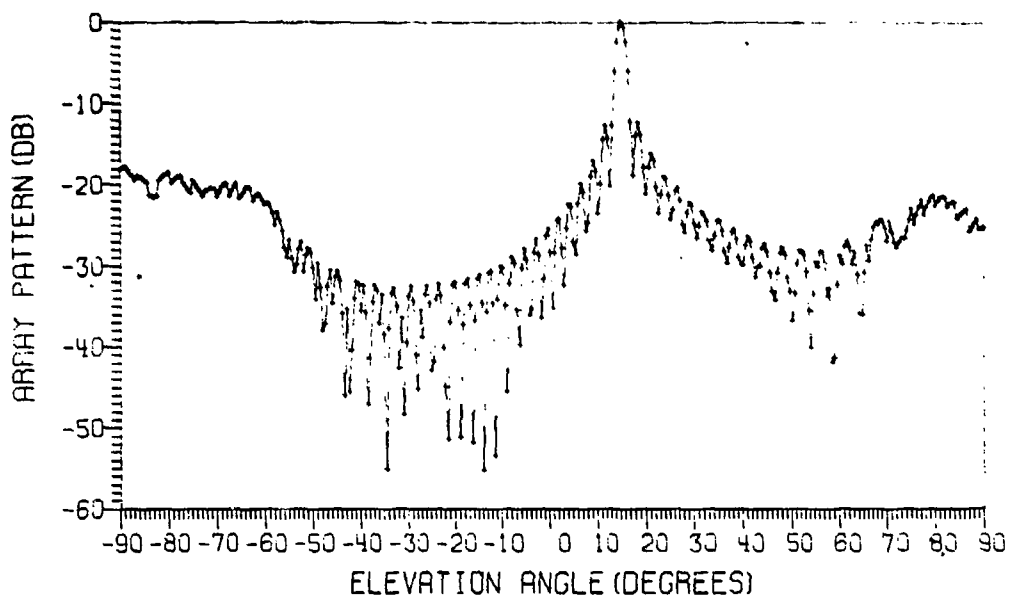
44

Fig. 20b — Elevation pattern of 48 X 1 TMS array, projected uniformly spaced around
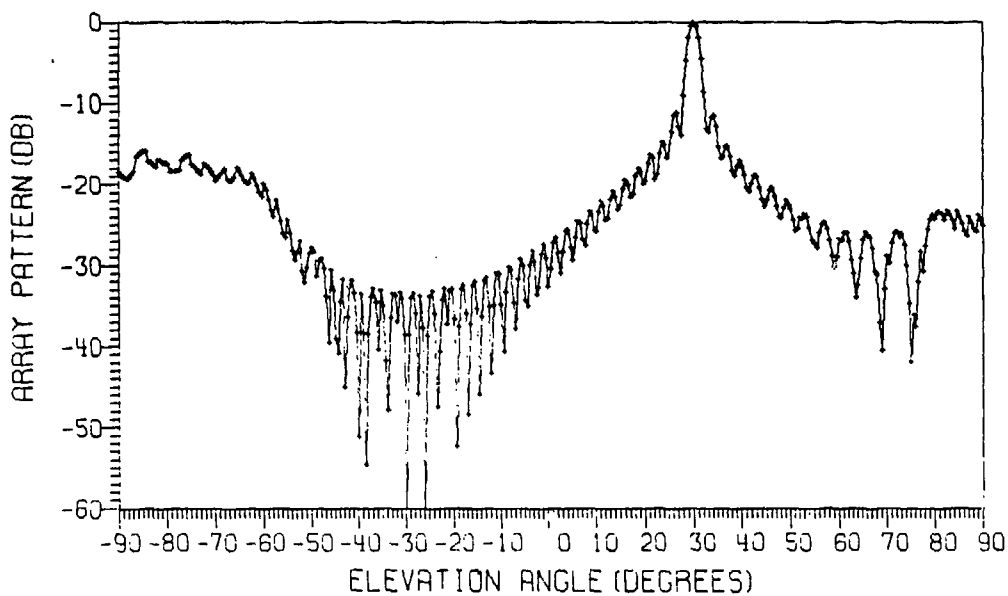fuselage and scanned to 15° in elevation applying exact steering phase

Fig. 20c — Elevation pattern of 48 X 1 TMS array, projected uniformly spaced around
fuselage and scanned to 30° in elevation applying exact steering phase

45

Projected uniformly spaced array with linear array phasing — The element distribution was assumed to be the same as in the preceding paragraph. However, instead of using exact steering phase for scanning, a linear array phasing was used. The corresponding radiation patterns for 0°, 15°, and 30° elevation scan angles are shown in Figs. 21a through 21c. Comparing these with the patterns for Figs. 20a through 20c indicates that the approximate phase approach degrades the pattern even at 15° scan. For 30° scan (Fig. 21c), the beamwidth becomes too wide with corresponding loss in gain. These degradations are caused by the increased phase errors as the array arc angle and scan angle are increased, as discussed earlier. Therefore, the approximate phasing may not be used with a 48-element array. However, it is doubtful if a 48-element array can be accommodated on the fuselage of P-3 aircraft.

Summary of TMS Array on Fuselage — TMS arrays with 32 and 48 elements in the elevation plane were analyzed. For the scan range of ±15°, an approximate phasing can be used for a 32-element array with negligible degradation in array performance. For larger scan angles or for larger arrays, the row-column steering cannot be used. For such arrays a modification of the approximate phasing may be used, as discussed briefly. This approach is still under investigation at NRL.
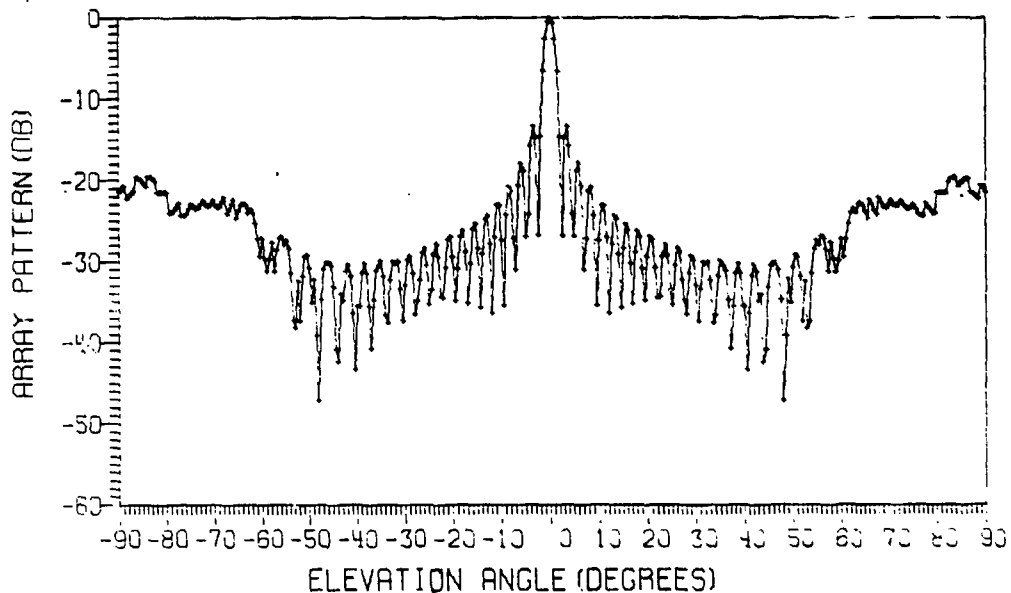

Fig. 21a — Elevation pattern of 48 × 1 TMS array, projected uniformly spaced around fuselage
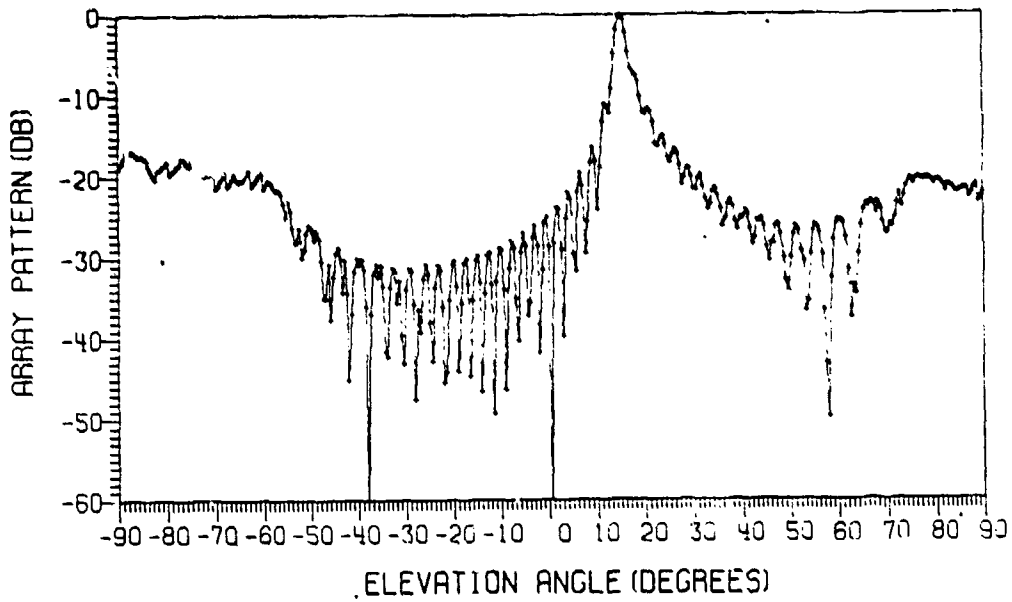
Fig. 21b — Elevation pattern of 48 X 1 TMS array, projected uniformly spaced around
fuselage and scanned to 15° in elevation applying linear array phasing
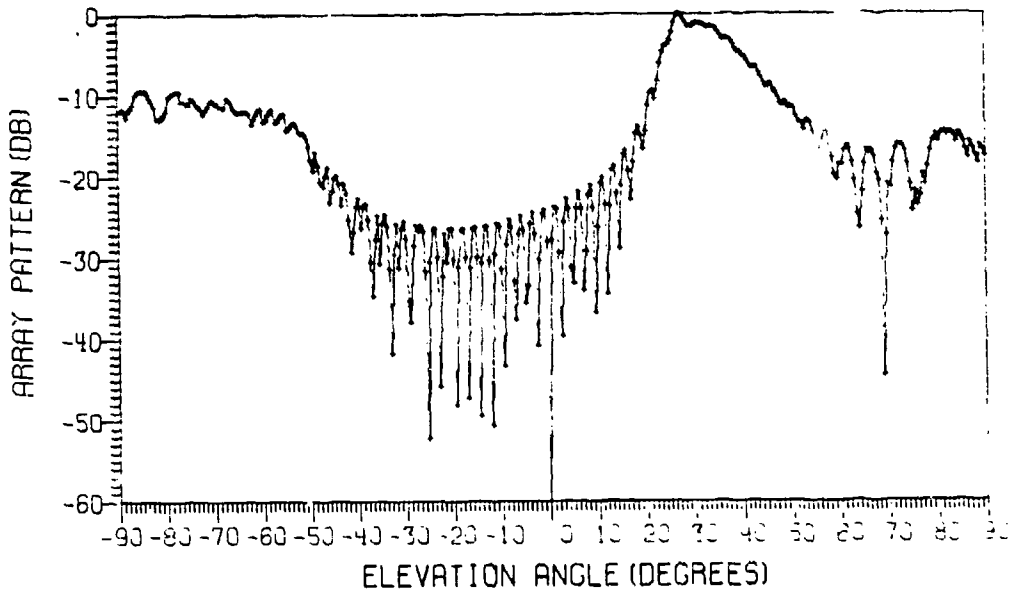

Fig. 21c — Elevation pattern of 48 X 1 TMS array, projected uniformly spaced around
fuselage and scanned to 30° in elevation applying linear array phasing

ARRAYS ON VERTICAL STABILIZER

To accommodate a TMS array on the fuselage of P-3 aircraft, it may be necessary to locate EATS and TCS arrays on the vertical stabilizer. If the vertical stabilizer surface is specified, the computer program discussed in Appendix A can be used to analyze the arrays on the vertical stabilizer. The exact description of the vertical stabilizer surface was not obtainable. Hence, an approximate approach was used taking the available data [1]. The vertical stabilizer surface, where the arrays may be located, can be approximated as a part of a large conical surface. The conical surface is defined by a base radius of curvature of 15 ft and cone angle of 7°, as shown in Fig. 22. To avoid the scattering effects of fuselage, the elements of the arrays on vertical stabilizer are assumed to be vertical dipoles. This will have the effect of reducing the side lobes in the elevation patterns.
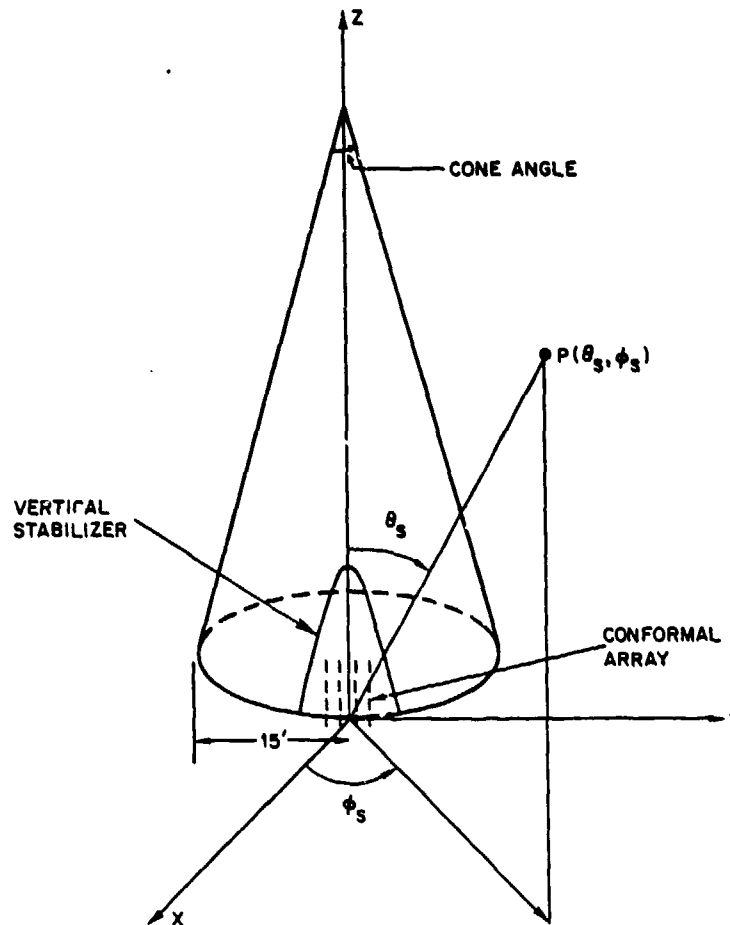

Fig. 22 — Geometry of a conformal array
on the vertical stabilizer

EATS Array

The EATS array on the vertical stabilizer is assumed to have seven rows and each row contains 13 elements. The arc length of the bottom row is assumed to be 6λ (1 m). The arc angle occupied by the array is found to be 2.5°. The EATS array and one side of the vertical stabilizer are shown in Fig. 22 as a part of a large conical surface. The computed radiation patterns are shown in Figs. 23a through 23e. Figures 23a through 23c are azimuth patterns for azimuth scan angles of 0°, 30°, and 60°. Since the array surface is conical, there is a cross-polarization component. However, since the vertical stabilizer surface is almost planar, the cross-polarization component is very small and is at least 20 dB below the main polarization component. The side lobes are below 20 dB except when the beam is scanned to 60°, where they are increased to about -10 dB. Figs. 23d and 23e show the elevation patterns for elevation scan angles of 0° and 15°, respectively. As expected, the side lobes are very low.
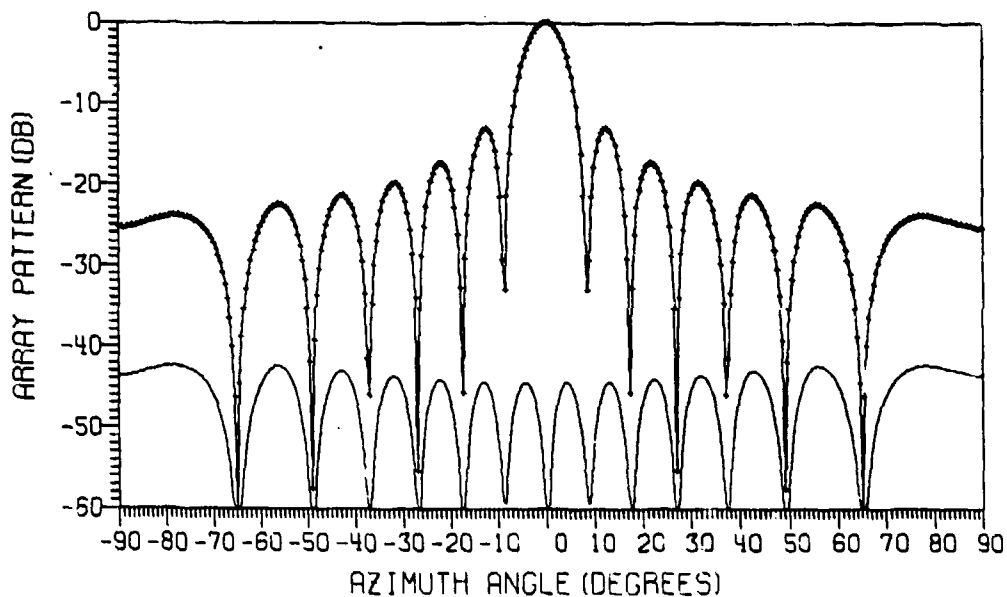

Fig. 23a — Azimuth pattern of 7 X 13 EATS array located on vertical stabilizer
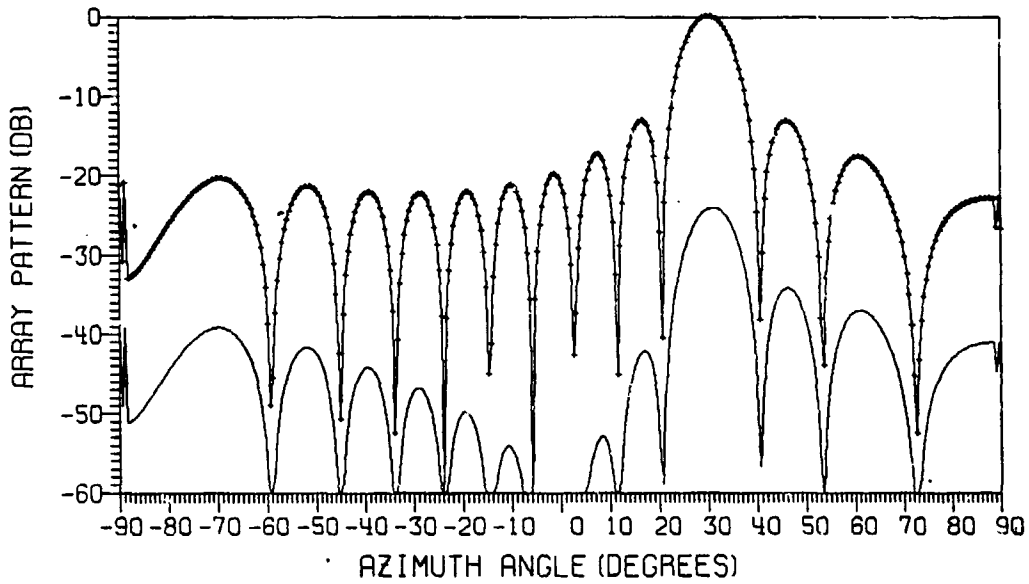
Fig. 23b — Azimuth pattern of 7 X 13 EATS array located on vertical stabilizer and scanned to 30° in azimuth applying exact phasing
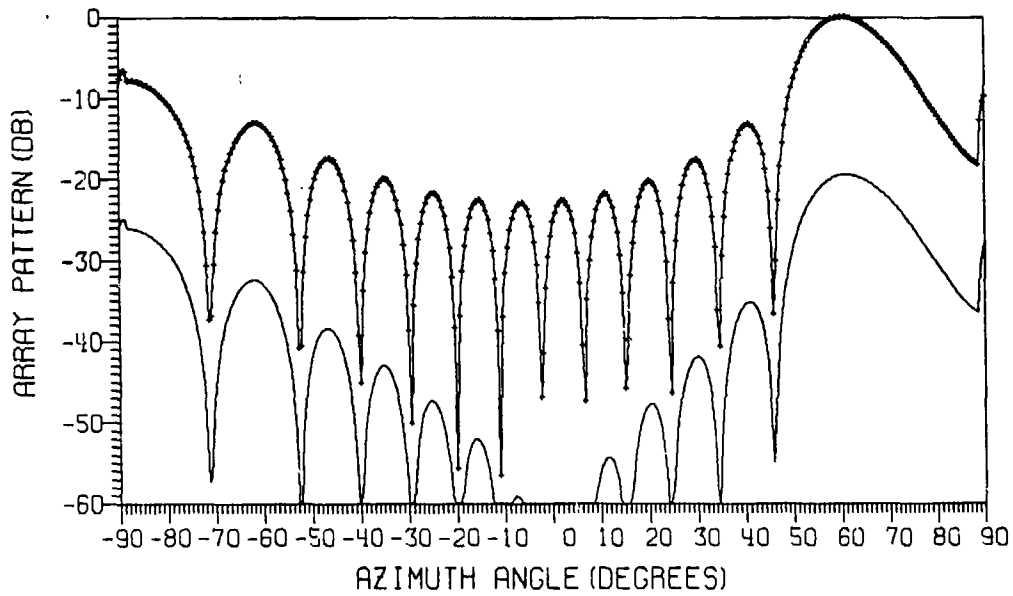

Fig. 23c — Azimuth pattern of 7 X 13 EATS array located on vertical stabilizer and scanned to 60° in azimuth applying exact phasing
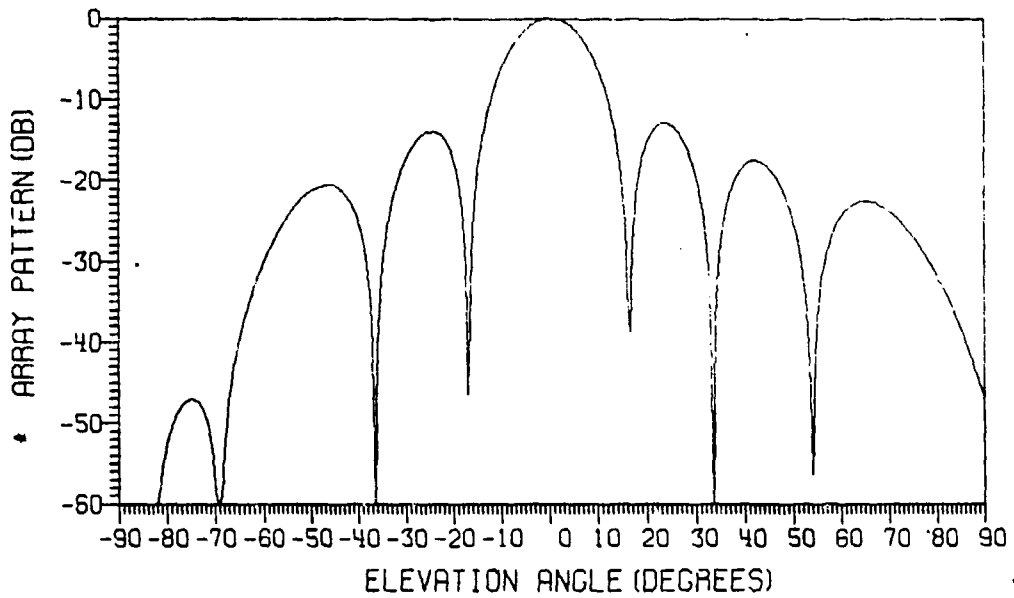
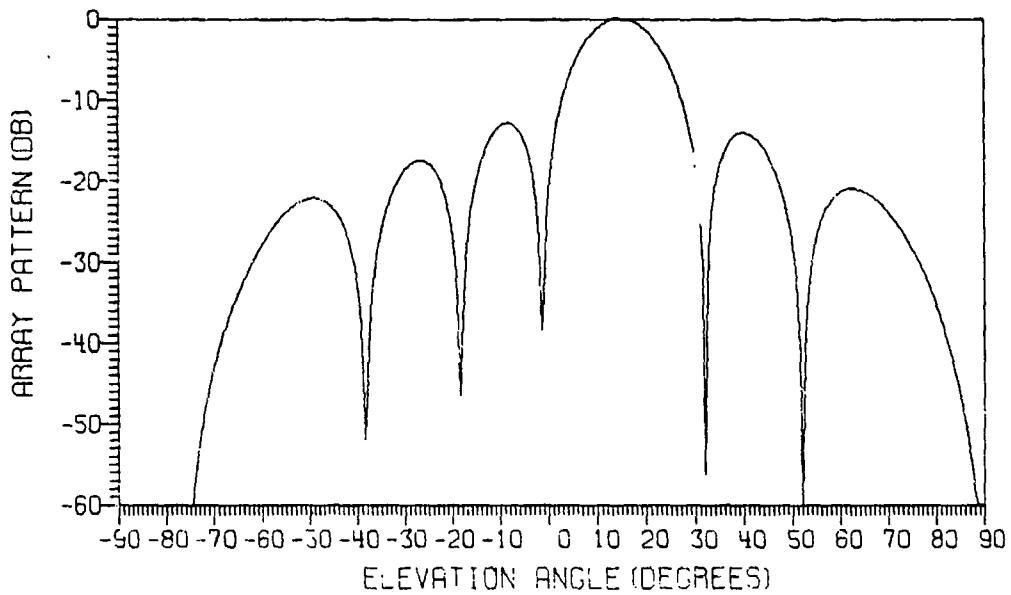Fig. 23c — Elevation pattern of 7 X 13 EATS array located on vertical stabilizer

Fig. 23e — Elevation pattern of 7 X 13 EATS array located on vertical stabilizer and scanned to 15° in elevation applying exact phasing

TCS Array

The TCS array on the vertical stabilizer is assumed to have 20 rows, and each row contains 40 elements. The arc length of the bottom row is assumed to be 19.5λ at 4.4 GHz. The arc angle occupied by the array is found to be 1.6°. The computed radiation patterns are shown in Figs. 24a through 24e. From these figures, it is observed that the conclusions reached for an EATS array will also apply for a TCS array except that the side lobes are about -20 dB for a TCS array as compared to -10 dB for an EATS array when scanned to 60° in azimuth plane.
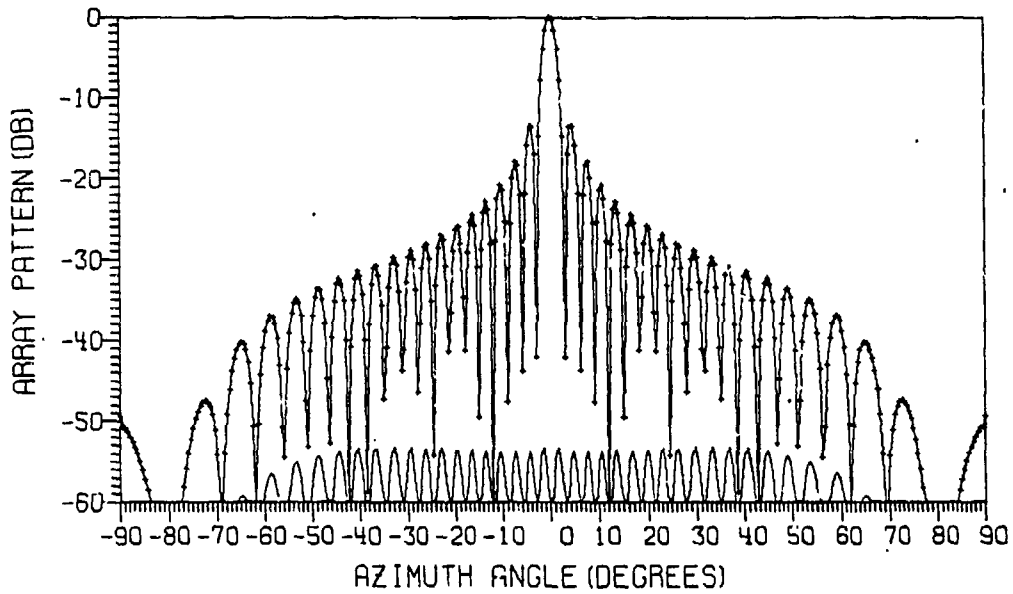

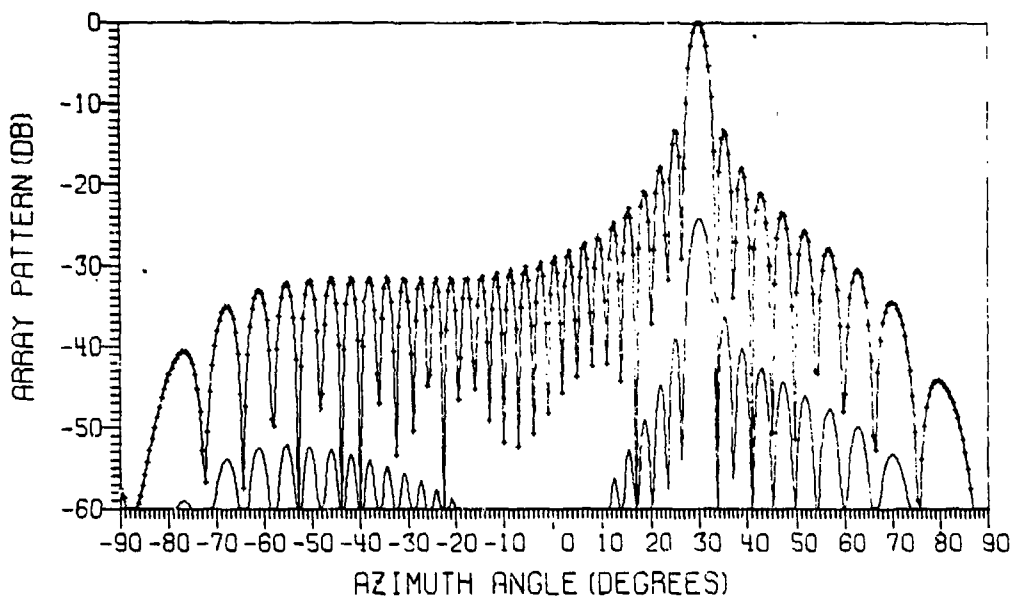Fig. 24a — Azimuth pattern of 20 X 40 TCS array located on vertical stabilizer

Fig. 24b — Azimuth pattern of 20 X 40 TCS array located on vertical stabilizer and scanned to 30° in azimuth applying exact phasing

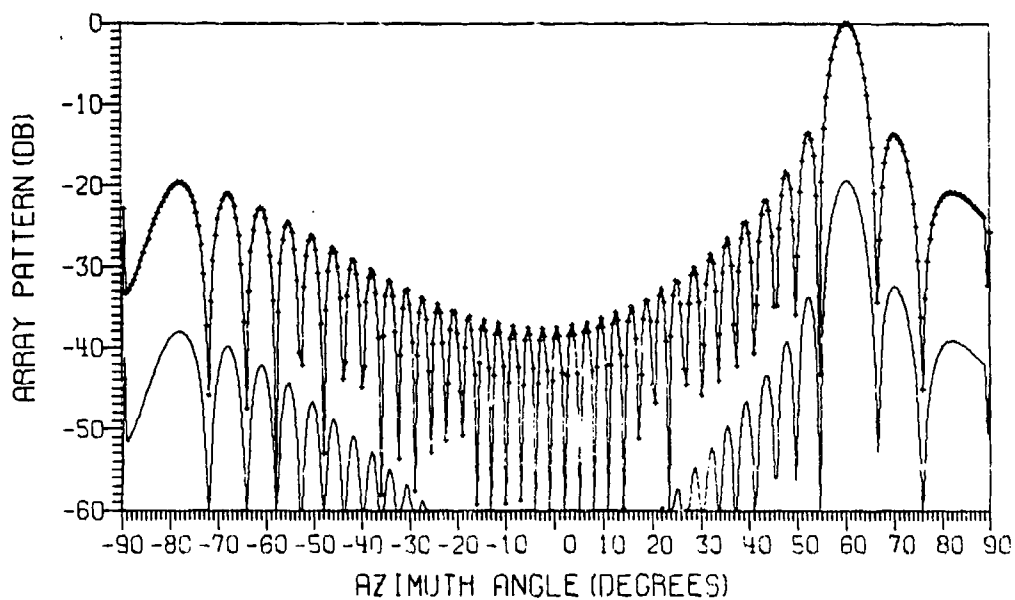Fig. 24c — Azimuth pattern of 20 X 40 TCS array located on vertical stabilizer and scanned to 60° in azimuth applying exact phasing

ELEVATION ANGLE (DEGREES)
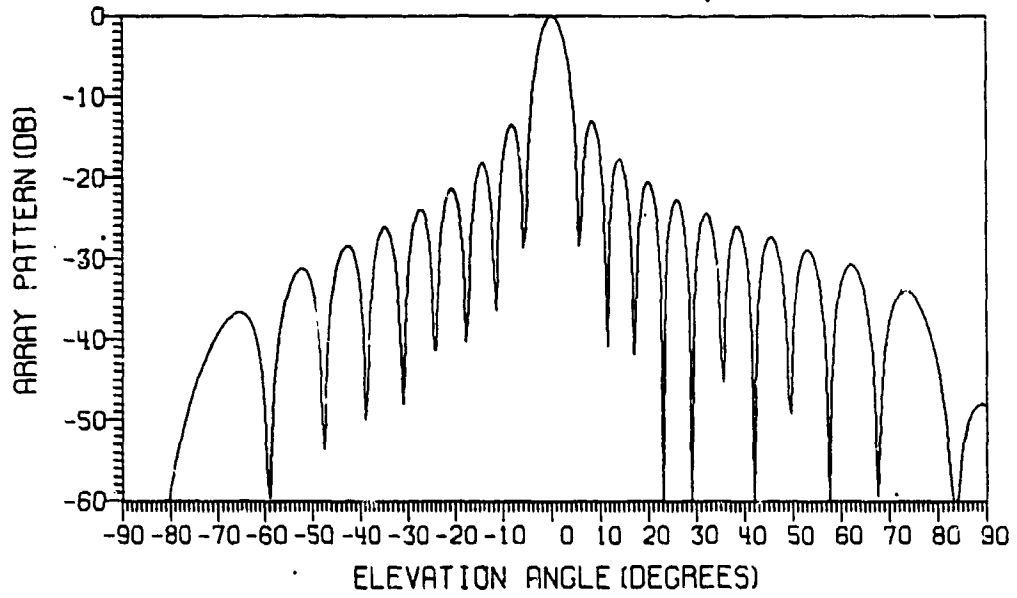
Fig. 24d — Elevation pattern of 20 X 40 TCS array located on vertical stabilizer
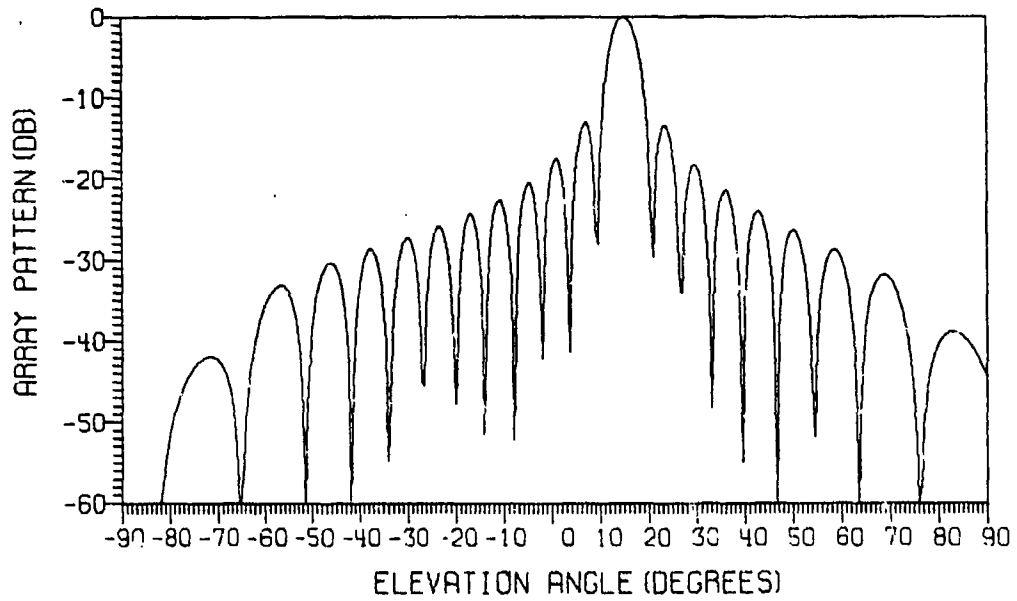

ELEVATION ANGLE (DEGREES)

Fig. 24e — Elevation pattern of 20 X 40 TCS array located on vertical stabilizer and scanned to 15° in elevation applying exact phasing

Summary of the Arrays on Vertical Stabilizer

The vertical stabilizer is approximated as a part of a large conical surface. Therefore, the radiation fields contained some cross-polarization components. However, the radius of curvature is very large, and the arc angle occupied by the arrays is small. This resulted in a very small cross-polarization. The radiation pattern can be shown to be very similar to planar arrays of the same size. Therefore, the approximate phasing method can be used for the arrays on the vertical stabilizer with negligible degradation in array performance.

CONCLUSIONS

A general computer program was developed to analyze the performance of conformal arrays. The EATS and TCS arrays were analyzed as located on the fuselage or vertical stabilizer of P-3 aircraft. A simple phase steering technique is recommended to simplify the hardware required to scan the conformal arrays. When this technique is applied to EATS and TCS arrays, it is shown that the row-column steering is cost effective with negligible degradation in array performance. This simpler phasing method could also be used for TMS arrays of 32 elements in the elevation plane. For larger TMS arrays or wider scanning (scanning to 60° in azimuth), the simpler phase steering method results in large phase errors. For such arrays, a modification of the simpler phase steering method is suggested. When TMS arrays are located on the fuselage, it may be necessary to locate EATS and TCS arrays on the vertical stabilizer. Therefore, such arrays were analyzed. It is suggested that the simpler row-column steering be used for such arrays with negligible degradation in array performance.

REFERENCES

1. "Handbook, Structural Repair Instructions for Navy Models P-3A, P-3B and P-3C Aircraft," NAVAIR Systems Command, NAVAIR 01-75PAA-3-1, Dec. 1, 1971.

2. J.F. Cline and J.P. McHenry, "System Requirements for Extended Area Tracking, Target Control, and Telemetry at the Pacific Missile Range," Stanford Research Institute Research Memorandum RM-314, July 1973.

3. E.D. Sharp, "A Triangular Arrangement of Planar-Array Elements that Reduces the Number Needed," IRE Trans., AP-9, 126-129 (March 1961).

Appendix A

BRIEF DESCRIPTION OF GENERAL COMPUTER PROGRAM

For the purpose of this report, a brief description of a computer program developed to find the radiation patterns of conformal arrays located on a general surface will be given. The detailed description, together with the written program, will be published as a separate report. By supplying proper input cards and the subroutines, users can apply the program to the arrays on a general conformal surface, a parabolic cylinder, a circular torus, a cone, and a planar surface.

In the case of a general conformal surface, each element position and its orientation are supplied as inputs to the program. The element position is supplied as three components in a rectangular coordinate system with respect to a reference point on the array. The element orientation is expressed by three angles measured from array broadside. For circular cylinder, circular torus, and planar surfaces, the number of elements, the array aperture, and the radius of curvature in x and y directions must be specified. For a planar surface the radius of curvature is specified as zero. For conical surface, the number of rows, the base radius of curvature, the array arc angle, the cone angle, the spacing between the rows and the interelement spacing along the base must be specified.

In all cases, the element pattern can be specified as a horizontal or a vertical dipole. In addition, an exact phase or an approximate phase (row-column steering) can be selected for scanning the beam. Array patterns can be obtained for any polar angle cuts over an angular range of $\pm 90°$. The computer gives a printed output and a plot of the radiation patterns. Cross-polarization component, if any, will be plotted on the same curve. The radiation patterns presented in this report are the examples of the output expected.